Electronic Supplementary Information

# Anion transport across varying lipid membranes – the effect of lipophilicity

Michael J. Spooner and Philip A. Gale*

* Chemistry, University of Southampton, Southampton SO17 1BJ, UK. E-mail: philip.gale@soton.ac.uk; Fax: +44 (0)2380 596805; Tel: +44 (0)2380 593332

## Table of Contents

# 1 Synthesis

NMR spectra were recorded on Bruker AVII400 or Bruker AVIIIHD400 FT-NMR spectrometers in the indicated solvent at 298 K. Chemical shifts for proton and carbon spectra are reported on the delta scale in ppm and were referenced to residual solvent references or internal TMS reference. High resolution mass spectra were recorded using positive/negative ion electrospray ionisation and analysed using a MaXis (Bruker Daltonics, Bremen, Germany) mass spectrometer equipped with a Time of Flight (TOF) analyser. Samples were introduced to the mass spectrometer via a Dionex Ultimate 3000 autosampler and uHPLC pump. Gradient 20% acetonitrile (0.2% formic acid) to 100% acetonitrile (0.2% formic acid ) in five minutes at 0.6 mL min. Column, Acquity UPLC BEH C18 (Waters) 1.7 micron 50 x 2.1mm. Starting materials were used as provided by suppliers. Dichloromethane was distilled over sodium hydroxide under nitrogen before use. Other solvents were used without further purification. Compounds **1**[1], **2**[1], **3**[2] & **10**[3] have been previously reported.

## 1.1 1-phenyl-3-ethylthiourea (1)

Aniline (2.5 mmol) was dissolved in pyridine (10 ml) under nitrogen atmosphere. Ethyl isothiocyanate (2.5 mmol) was added and the pale yellow solution stirred at 80°C under nitrogen overnight. The volatiles were removed under reduced pressure yielding yellow oil.

The oil was dissolved in methanol and purified on an Isolute® SCX-2 cation-exchange column. The methanol phase was collected and the solvent removed, yielding colourless oil. The oil was purified by flash chromatography (ethyl acetate eluent) yielding a waxy white solid. The solid was further purified by crystallisation from chloroform/hexane, yielding white crystals.

Yield: 43 %. HRMS ESI$^+$ = $[C_9H_{13}N_2S]^+$: 181.0794 (calc), 181.0796 (found), -1.4 ppm (err); $[C_9H_{12}N_2SNa]^+$: 203.0613 (calc), 203.0616 (found), -1.5 ppm (err). $^1$H NMR (400 MHz, DMSO-$d_6$) δ 1.12 (t, *J*=7.15 Hz, 3H), 3.41-3.56 (m, 2H), 7.05-7.16 (m, 1H), 7.26-7.36 (m, 2H), 7.39 (d, *J*=8.10 Hz, 2H), 7.72 (br. s., 1H), 9.43 (br. s., 1H). $^{13}$C NMR (101 MHz, DMSO-$d_6$) δ 14.7, 39.2, 123.6, 124.5, 129.1, 139.7, 180.5. Melting point: 99.6 – 100.4°C.

## 1.2 1-(p-tolyl)-3-ethylthiourea (2)

p-Toluidine (2.5 mmol) was dissolved in pyridine (10 ml) under nitrogen atmosphere. Ethyl isothiocyanate (2.5 mmol) was added and the orange solution stirred at 80°C under nitrogen overnight. The volatiles were removed under reduced pressure yielding brown oil.

The oil was dissolved in methanol and purified on an Isolute® SCX-2 cation-exchange column. The methanol phase was collected and the solvent removed, yielding an off-white solid. The solid was purified by flash chromatography (3:1 Ethyl Acetate:Hexane eluent) yielding a waxy white solid. The solid was further purified by crystallisation from chloroform/hexane, yielding white, needle-like crystals.

Yield: 21 %. HRMS ESI$^+$ = $[C_{10}H_{15}N_2S]^+$: 195.0950 (calc), 195.0949 (found), 0.9 ppm (err); $[C_{10}H_{14}N_2SNa]^+$: 217.0770 (calc), 217.0769 (found), 0.3 ppm (err). $^1$H NMR (400 MHz, DMSO-$d_6$) δ 1.10 (t, *J*=7.15 Hz, 3H), 2.27 (s, 3H), 3.41-3.52 (m, 2H), 7.10-7.15 (m, *J*=8.31 Hz, 2H), 7.23 (d, *J*=8.31 Hz, 2H), 7.59 (br. s., 1H), 9.32 (br. s., 1H). $^{13}$C NMR (101 MHz, DMSO-$d_6$) δ 14.7, 21.0, 39.2, 124.1, 129.6, 133.9, 137.0, 180.6. Melting point: 99.9 – 100.8°C.

## 1.3 1-(4-ethylphenyl)-3-ethylthiourea (3)

4-ethylaniline (2.5 mmol) was dissolved in pyridine (10 ml) under nitrogen atmosphere. Ethyl isothiocyanate (2.5 mmol) was added and the orange solution stirred at 80°C under nitrogen overnight. The volatiles were removed under reduced pressure yielding brown oil.

The oil was dissolved in methanol and purified on an Isolute® SCX-2 cation-exchange column. The methanol phase was collected and the solvent removed, yielding a waxy yellow solid. The solid was purified by flash chromatography (3:1 Ethyl Acetate:Hexane eluent) yielding a waxy off-white solid. The solid was further purified by crystallisation from chloroform/hexane, yielding white crystals.

Yield: 42 %. HRMS ESI$^+$ = $[C_{11}H_{17}N_2S]^+$: 209.1107 (calc), 209.1106 (found), 0.6 ppm (err); $[C_{11}H_{16}N_2SNa]^+$: 231.0926 (calc), 231.0928 (found), -0.7 ppm (err) ; $[C_{22}H_{32}N_4S_2Na]^+$: 439.1961 (calc), 439.1965 (found), -0.9 ppm (err). $^1$H NMR (400 MHz, DMSO-$d_6$) δ 1.04-1.13 (m, 3H), 1.13-1.20 (m, 3H), 2.52-2.61 (m, 2H), 3.46 (d, *J*=5.50 Hz, 2H), 7.16 (d, *J*=8.19 Hz, 2H), 7.21-7.27 (m, 2H), 7.61 (br. s., 1H), 8.81-9.54 (m, 1H). $^{13}$C NMR (101 MHz, DMSO-$d_6$) δ 14.7, 16.1, 28.1, 39.2, 124.0, 128.4, 137.2, 140.2, 180.5. Melting point: 89.9 – 90.5°C.

## 1.4 1-(4-ethylphenyl)-3-propylthiourea (4)

4-ethylaniline (2.5 mmol) was dissolved in dry DCM (6 ml) under nitrogen atmosphere. Propyl isothiocyanate (2.5 mmol) was added and the orange solution stirred under nitrogen overnight. The volatiles were removed under reduced pressure yielding a yellow solid.

The solid was dissolved in methanol and purified on an Isolute® SCX-2 cation-exchange column. The methanol phase was collected and the solvent removed, yielding a waxy yellow solid. The solid was purified by flash chromatography (diethyl ether eluent) yielding a waxy white solid.

Yield: 11 %. HRMS ESI$^+$ = $[C_{12}H_{19}N_2S]^+$: 223.1263 (calc), 223.1266 (found), -1.3 ppm (err). $^1$H NMR (400 MHz, DMSO-$d_6$) δ 0.93 (t, *J*=7.40 Hz, 3H), 1.23 (t, *J*=7.58 Hz, 3H), 1.54-1.65 (m, *J*=7.31, 7.31, 7.31, 7.31, 7.31 Hz, 2H), 2.60-2.66 (m, 2H), 3.42-3.52 (m, *J*=5.62 Hz, 2H), 7.21 (d, *J*=8.31 Hz, 2H), 7.27-7.37 (m, *J*=8.31 Hz, 2H), 7.69 (br. s., 1H), 9.39 (br. s., 1H). $^{13}$C NMR (101 MHz, DMSO-$d_6$) δ 11.9, 16.1, 22.3, 28.1, 46.1, 123.9, 128.4, 137.3, 140.2, 180.8. Melting point: 71.7 – 71.8°C.

## 1.5 1-(4-propylphenyl)-3-propylthiourea (5)

4-propylaniline (2.5 mmol) was dissolved in pyridine (10 ml) under nitrogen atmosphere. Propyl isothiocyanate (2.5 mmol) was added and the solution stirred at 80°C under nitrogen overnight. The volatiles were removed under reduced pressure yielding brown oil.

The oil was dissolved in methanol and purified on an Isolute® SCX-2 cation-exchange column. The methanol phase was collected and the solvent removed, yielding colourless oil. The oil was purified by flash chromatography (1$^{st}$ elution DMC, second diethyl ether) yielding a waxy off-white solid. The solid was further purified by crystallisation from methanol/water, yielding a white solid.

Yield: 30 %. HRMS ESI$^+$ = $[C_{13}H_{21}N_2S]^+$: 237.1420 (calc), 237.1419 (found), 0.5 ppm (err); $[C_{13}H_{20}N_2SNa]^+$: 259.1239 (calc), 259.1240 (found), -0.1 ppm (err). $^1$H NMR (400 MHz, DMSO-$d_6$) δ 0.83-0.95 (m, 7H), 1.56 (dsxt, 4H), 2.48-2.51 (m, 1H), 2.54 (s, 1H), 3.37-3.47 (m, 2H), 7.09-7.18 (m, *J*=8.31 Hz, 2H), 7.27 (d, *J*=8.31 Hz, 2H), 7.64 (br. s., 1H), 9.34 (br. s., 1H). $^{13}$C NMR (101 MHz, DMSO-$d_6$) δ 11.9, 14.2, 22.3, 24.6, 37.2, 46.1, 123.7, 128.9, 137.3, 138.6, 180.8. Melting point: 71.1 – 71.8°C.

## 1.6 1-(4-propylphenyl)-3-butylthiourea (6)

4-propylaniline (2.5 mmol) was dissolved in dry DCM (6 ml) under nitrogen atmosphere. Butyl isothiocyanate (2.5 mmol) was added and the yellow solution stirred under nitrogen overnight. The volatiles were removed under reduced pressure yielding cloudy oil.

The oil was dissolved in methanol and purified on an Isolute® SCX-2 cation-exchange column. The methanol phase was collected and the solvent removed, yielding colourless oil. The oil was purified by flash chromatography (1:1 diethyl ether:hexane eluent) yielding a waxy white solid.

Yield: 19 %. HRMS ESI$^+$ = $[C_{14}H_{23}N_2S]^+$: 251.1576 (calc), 251.1582 (found), -2.1 ppm (err). $^1$H NMR (400 MHz, DMSO-$d_6$) δ 0.86-0.94 (m, 6H), 1.31 (qt, *J*=14.92, 7.38 Hz, 2H), 1.47-1.63 (m, 4H), 2.53-2.56 (m, 1H), 3.45 (d, *J*=5.62 Hz, 2H), 7.11-7.16 (m, *J*=8.31 Hz, 2H), 7.27 (d, *J*=8.44 Hz, 2H), 7.61 (br. s., 1H), 9.32 (br. s., 1H). $^{13}$C NMR (101 MHz, DMSO-$d_6$) δ 14.2, 14.2, 20.1, 24.6, 31.1, 37.2, 44.0, 123.7, 128.9, 180.7. Melting point: 54.9 – 55.7°C.

## 1.7 1-(4-butylphenyl)-3-butylthiourea (7)

4-butylaniline (2.5 mmol) was dissolved in pyridine (10 ml) under nitrogen atmosphere. Butyl isothiocyanate (2.5 mmol) was added and the brown solution stirred at 80°C under nitrogen overnight. The volatiles were removed under reduced pressure yielding brown oil.

The oil was dissolved in methanol and purified on an Isolute® SCX-2 cation-exchange column. The methanol phase was collected and the solvent removed, yielding colourless oil. The oil was purified by flash chromatography (1$^{st}$ elution DMC, second diethyl ether) yielding a waxy off-white solid. The solid was further purified by crystallisation from methanol/water, yielding a white solid.

Yield: 28 %. HRMS ESI$^+$ = $[C_{15}H_{25}N_2S]^+$: 265.1733 (calc), 265.1728 (found), 1.7 ppm (err); $[C_{15}H_{24}N_2SNa]^+$: 287.1552 (calc), 287.1547 (found), 1.8 ppm (err). $^1$H NMR (400 MHz, DMSO-$d_6$) δ 0.86-0.94 (m, 6H), 0.90 (t, *J*=7.40 Hz, 6H), 1.25-1.37 (m, 4H), 1.31 (dq, *J*=14.86, 7.36 Hz, 4H), 1.46-1.59 (m, 4H), 1.47-1.58 (m, 4H), 3.45 (d, *J*=5.26 Hz, 2H), 3.39-3.51 (m, 2H), 7.13 (d, *J*=8.31 Hz, 2H), 7.09-7.17 (m, 2H), 7.26 (d, *J*=8.31 Hz, 2H), 7.23-7.30 (m, 2H), 7.47-7.70 (m, 1H), 7.61 (br. s., 1H), 9.32 (br. s., 1H), 9.21-9.42 (m, 1H). $^{13}$C NMR (101 MHz, DMSO-$d_6$) δ 14.2, 14.3, 20.1, 22.2, 31.1, 33.6, 34.7, 44.0, 123.7, 128.8, 137.3, 138.7, 180.8. Melting point: 57.8 – 58.2°C.

## 1.8 1-(4-butylphenyl)-3-pentylthiourea (8)

4-butylaniline (2.5 mmol) was dissolved in dry DCM (6 ml) under nitrogen atmosphere. Pentyl isothiocyanate (2.5 mmol) was added and the orange solution stirred under nitrogen overnight. The volatiles were removed under reduced pressure yielding orange oil.

The oil was dissolved in methanol and purified on an Isolute® SCX-2 cation-exchange column. The methanol phase was collected and the solvent removed, yielding a yellow solid. The solid was purified by flash chromatography (2:1 diethyl ether:hexane eluent) yielding a waxy white solid.

Yield: 24 %. HRMS ESI$^+$ = $[C_{16}H_{27}N_2S]^+$: 279.1889 (calc), 279.1892 (found), -1.0 ppm (err). $^1$H NMR (400 MHz, DMSO-$d_6$) δ 0.83-0.96 (m, 6H), 1.22-1.38 (m, 7H), 1.47-1.60 (m, 4H), 2.54 (t, *J*=7.64 Hz, 2H), 3.38-3.50 (m, 2H), 7.13 (d, *J*=8.31 Hz, 2H), 7.23-7.31 (m, *J*=8.31 Hz, 2H), 7.61 (br. s., 1H), 9.32 (br. s., 1H). $^{13}$C NMR (101 MHz, DMSO-$d_6$) δ 14.3, 14.4, 22.2, 22.4, 28.7, 29.1, 33.6, 34.8, 44.3, 123.7, 128.9, 137.3, 138.7, 180.7. Melting point: 53.9 – 54.4°C.

## 1.9 1-(4-pentylphenyl)-3-pentylthiourea (9)

4-pentylaniline (2.5 mmol) was dissolved in dry DCM (6 ml) under nitrogen atmosphere. Pentyl isothiocyanate (2.5 mmol) was added and the pale yellow solution stirred under nitrogen overnight. The volatiles were removed under reduced pressure yielding an off-white solid.

The solid was dissolved in methanol and purified on an Isolute® SCX-2 cation-exchange column. The methanol phase was collected and the solvent removed, yielding an off-white solid. The solid was purified by flash chromatography (2:1 diethyl ether:hexane eluent) yielding a waxy white solid.

Yield: 18 %. HRMS ESI$^+$ = $[C_{17}H_{29}N_2S]^+$: 293.2046 (calc), 293.2048 (found), -0.8 ppm (err). $^1$H NMR (400 MHz, DMSO-$d_6$) δ 0.88 (d, *J*=7.09 Hz, 5H), 1.21-1.37 (m, 9H), 1.47-1.62 (m, 4H), 3.38-3.51 (m, 2H), 7.13 (d, *J*=8.44 Hz, 2H), 7.22-7.30 (m, *J*=8.44 Hz, 2H), 7.61 (br. s., 1H), 9.33 (br. s., 1H). $^{13}$C NMR (101

MHz, DMSO-$d_6$) δ 14.4, 22.4, 22.4, 28.7, 29.1, 31.1, 31.4, 35.0, 44.3, 123.7, 128.9, 137.3, 138.8, 180.7. Melting point: 55.6 – 56.6°C.

## 1.10 1-(4-pentylphenyl)-3-hexylthiourea (10)

4-pentylaniline (2.5 mmol) was dissolved in dry DCM (6 ml) under nitrogen atmosphere. Hexyl isothiocyanate (2.5 mmol) was added and the pale yellow solution stirred under nitrogen overnight. The volatiles were removed under reduced pressure yielding yellow oil.

The oil was dissolved in methanol and purified on an Isolute® SCX-2 cation-exchange column. The methanol phase was collected and the solvent removed, yielding a yellow solid. The solid was purified by flash chromatography (2:1 diethyl ether:hexane eluent) yielding a waxy white solid.

Yield: 22 %. HRMS ESI$^+$ = $[C_{18}H_{31}N_2S]^+$: 307.2202 (calc), 307.2203 (found), -0.3 ppm (err). $^1$H NMR (400 MHz, DMSO-$d_6$) δ 0.82-0.93 (m, 7H), 1.23-1.35 (m, 11H), 1.46-1.62 (m, 4H), 3.38-3.50 (m, 2H), 7.09-7.17 (m, *J*=8.44 Hz, 2H), 7.26 (d, *J*=8.31 Hz, 2H), 7.60 (br. s., 1H), 9.33 (br. s., 1H). $^{13}$C NMR (101 MHz, DMSO-$d_6$) δ 14.4, 22.4, 22.6, 26.6, 29.0, 31.2, 31.4, 31.5, 35.0, 44.3, 123.7, 128.9, 137.3, 138.7, 180.7. Melting point: 53.8 – 54.7°C.

## 1.11 1-(4-hexylphenyl)-3-hexylthiourea (11)

4-hexylaniline (2.5 mmol) was dissolved in pyridine (10 ml) under nitrogen atmosphere. Hexyl isothiocyanate (2.5 mmol) was added and the red solution stirred at 80°C under nitrogen overnight. The volatiles were removed under reduced pressure yielding orange oil.

The oil was dissolved in methanol and purified on an Isolute® SCX-2 cation-exchange column. The methanol phase was collected and the solvent removed, yielding a yellow solid. The solid was purified by flash chromatography (2:1 hexane:ethyl acetate) yielding a waxy yellow solid. The solid was further purified by crystallisation from methanol/water, yielding a white solid.

Yield: 67 %. HRMS ESI$^+$ = $[C_{19}H_{33}N_2S]^+$: 321.2359 (calc), 321.2363 (found), -1.3 ppm (err). $^1$H NMR (400 MHz, DMSO-$d_6$) δ 0.86 (q, *J*=6.81 Hz, 7H), 1.22-1.34 (m, 14H), 1.46-1.59 (m, 5H), 2.52-2.56 (m, 2H), 3.40-3.49 (m, 2H), 7.09-7.15 (m, *J*=8.31 Hz, 2H), 7.26 (d, *J*=8.44 Hz, 2H), 7.59 (br. s., 1H), 9.31 (br. s., 1H). $^{13}$C NMR (101 MHz, DMSO-$d_6$) δ 14.4, 14.4, 22.5, 26.6, 28.8, 28.9, 31.4, 31.5, 31.6, 35.1, 44.3, 123.7, 128.8, 137.2, 138.8, 180.7. Melting point: 45.9 – 47.4°C.

## 1.12 1-(4-hexylphenyl)-3-heptylthiourea (12)

4-hexylaniline (2.5 mmol) was dissolved in pyridine (10 ml) under nitrogen atmosphere. Heptyl isothiocyanate (2.5 mmol) was added and the red solution stirred at 80°C under nitrogen overnight. The volatiles were removed under reduced pressure yielding orange oil.

The oil was dissolved in methanol and purified on an Isolute® SCX-2 cation-exchange column. The methanol phase was collected and the solvent removed, yielding a yellow solid. The solid was purified by flash chromatography (2:1 hexane:ethyl acetate) yielding a waxy white solid on drying. The solid was further purified by crystallisation from methanol/water, yielding white crystals.

Yield: 90 %. HRMS ESI$^+$ = $[C_{20}H_{35}N_2S]^+$: 335.2515 (calc), 335.2524 (found), -2.4 ppm (err). $^1$H NMR (400 MHz, DMSO-$d_6$) δ 0.86 (d, *J*=4.65 Hz, 6H), 0.82-0.90 (m, 6H), 1.27 (br. s., 14H), 1.21-1.32 (m, 13H), 1.52 (br. s., 4H), 1.46-1.60 (m, 4H), 2.53 (d, *J*=7.83 Hz, 1H), 4.07-4.23 (m, 1H), 7.12 (d, *J*=8.19 Hz, 2H), 7.09-7.15 (m, 2H), 7.25 (d, *J*=7.70 Hz, 2H), 7.22-7.27 (m, 2H), 7.58 (br. s., 1H), 7.52-7.66 (m, 1H), 9.31 (br. s., 1H), 9.21-9.41 (m, 1H). $^{13}$C NMR (101 MHz, DMSO-$d_6$) δ 14.4, 14.4, 22.5, 22.5, 26.8, 28.8, 28.9, 29.0, 31.4, 31.6, 31.6, 31.7, 35.0, 44.4, 123.7, 123.7, 128.9, 128.9, 137.4. Melting point: 49.0 – 50.0°C.

## 1.13 1-(4-heptylphenyl)-3-heptylthiourea (13)

4-heptylaniline (2.5 mmol) was dissolved in pyridine (10 ml) under nitrogen atmosphere. Heptyl isothiocyanate (2.5 mmol) was added and the orange solution stirred at 80°C under nitrogen overnight. The volatiles were removed under reduced pressure yielding orange oil.

The oil was dissolved in methanol and purified on an Isolute® SCX-2 cation-exchange column. The methanol phase was collected and the solvent removed, yielding an off-white solid. The solid was purified by flash chromatography (2:1 hexane:ethyl acetate) yielding a waxy white solid on drying. The solid was further purified by crystallisation from methanol/water, yielding white crystals.

Yield: 35 HRMS ESI$^+$ = $[C_{21}H_{37}N_2S]^+$: 349.2672 (calc), 349.2676 (found), -1.2 ppm (err). $^1$H NMR (400 MHz, DMSO-$d_6$) δ 0.81-0.92 (m, 7H), 1.17-1.37 (m, 18H), 1.47-1.60 (m, 4H), 2.53-2.56 (m, 1H), 3.38-3.49 (m, 2H), 7.10-7.15 (m, *J*=8.44 Hz, 2H), 7.26 (d, *J*=8.31 Hz, 2H), 7.59 (br. s., 1H), 9.32 (br. s., 1H). $^{13}$C NMR (101 MHz, DMSO-$d_6$) δ 14.4, 22.5, 22.6, 26.9, 28.9, 29.0, 29.0, 29.1, 31.5, 31.7, 35.1, 44.3, 123.7, 128.8, 137.3, 138.8, 180.7. Melting point: 47.2 – 47.8°C.

## 1.14 1-(4-heptylphenyl)-3-octylthiourea (14)

4-heptylaniline (2.5 mmol) was dissolved in dry DCM (6 ml) under nitrogen atmosphere. Octyl isothiocyanate (2.5 mmol) was added and the orange solution stirred under nitrogen overnight. The volatiles were removed under reduced pressure yielding orange oil.

The oil was dissolved in methanol and purified on an Isolute® SCX-2 cation-exchange column. The methanol phase was collected and the solvent removed, yielding yellow oil. The oil was purified by flash chromatography (1:1 diethyl ether:hexane eluent) yielding a waxy white solid.

Yield: 9 %. HRMS ESI$^+$ = $[C_{22}H_{39}N_2S]^+$: 363.2828 (calc), 363.2836 (found), -2.0 ppm (err). $^1$H NMR (400 MHz, DMSO-$d_6$) δ 0.81-0.92 (m, *J*=6.79, 3.44, 3.44, 3.44 Hz, 7H), 1.28 (br. s., 22H), 1.40-1.64 (m, 5H), 2.53-2.56 (m, 4H), 3.43 (br. s., 3H), 7.09-7.16 (m, *J*=8.31 Hz, 2H), 7.26 (d, *J*=8.44 Hz, 2H), 7.61 (br. s., 1H), 9.34 (br. s., 1H). $^{13}$C NMR (101 MHz, DMSO-$d_6$) δ 14.4, 14.4, 22.6, 26.9, 29.0, 29.0, 29.1, 29.1, 29.2, 31.5, 31.7, 31.7, 35.1, 40.9, 44.3, 123.7, 123.9, 128.8, 138.8, 180.7. Melting point: 48.8 – 49.9°C.

## 1.15 1-(4-octylphenyl)-3-octylthiourea (15)

4-octylaniline (2.5 mmol) was dissolved in pyridine (10 ml) under nitrogen atmosphere. Octyl isothiocyanate (2.5 mmol) was added and the pale yellow solution stirred at 80°C under nitrogen overnight. The volatiles were removed under reduced pressure yielding brown oil.

The oil was dissolved in 3:1 methanol/chloroform and purified on an Isolute® SCX-2 cation-exchange column. The methanol phase was collected and the solvent removed, yielding an off-white solid. The solid was purified by flash chromatography (diethyl ether eluent) yielding a waxy white solid on drying. The solid was further purified by crystallisation from methanol/DCM, yielding a white solid.

Yield: 29 %. HRMS ESI$^+$ = $[C_{23}H_{41}N_2S]^+$: 377.2985 (calc), 377.2984 (found), 0.3 ppm (err); $[C_{23}H_{40}N_2SNa]^+$: 399.2804 (calc), 399.2806 (found), -0.4 ppm (err). $^1$H NMR (400 MHz, DMSO-$d_6$) δ 0.81-0.92 (m, 6H), 1.20-1.34 (m, 22H), 1.53 (d, *J*=5.75 Hz, 4H), 3.36-3.50 (m, 2H), 7.12 (d, *J*=8.31 Hz, 2H), 7.23-7.29 (m, *J*=8.31 Hz, 2H), 7.59 (br. s., 1H), 9.32 (br. s., 1H). $^{13}$C NMR (101 MHz, DMSO-$d_6$) δ 14.4, 22.6, 26.9, 29.0, 29.2, 29.2, 29.3, 31.5, 31.7, 31.8, 35.1, 44.3, 123.7, 128.8, 137.3, 138.7, 180.7. Melting point: 58.3 – 59.4°C.

# 2 NMR Spectra

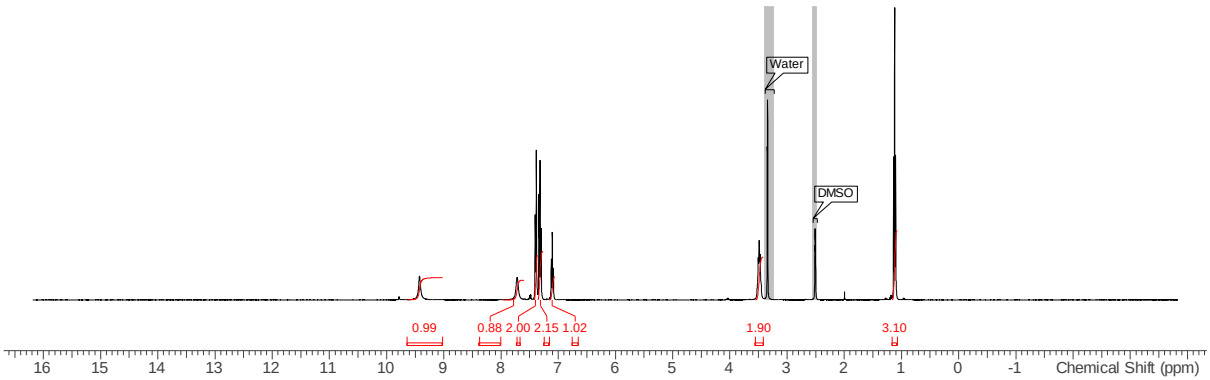


**Figure 1 -** $^{1}$H NMR (400 MHz, DMSO-$d_6$) spectrum of 1-phenyl-3-ethylthiourea.

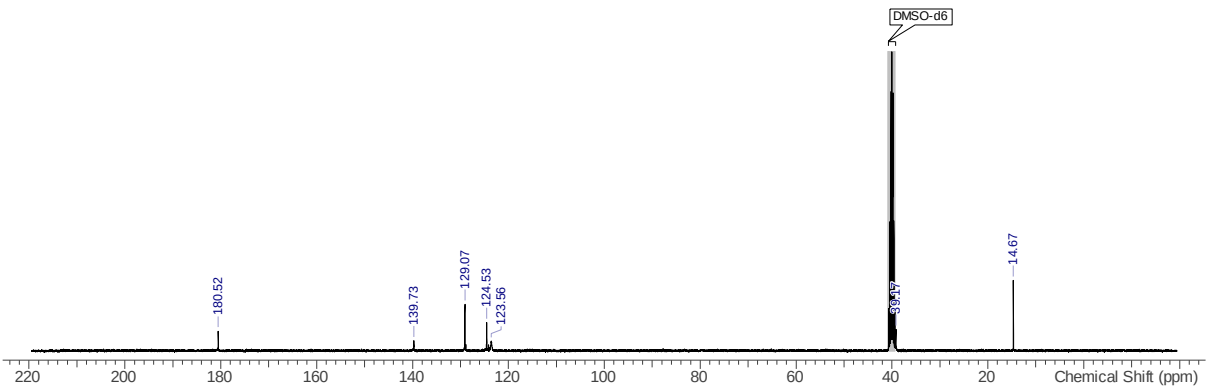


**Figure 2 -** $^{13}$C NMR (101 MHz, DMSO-$d_6$) spectrum of 1-phenyl-3-ethylthiourea.

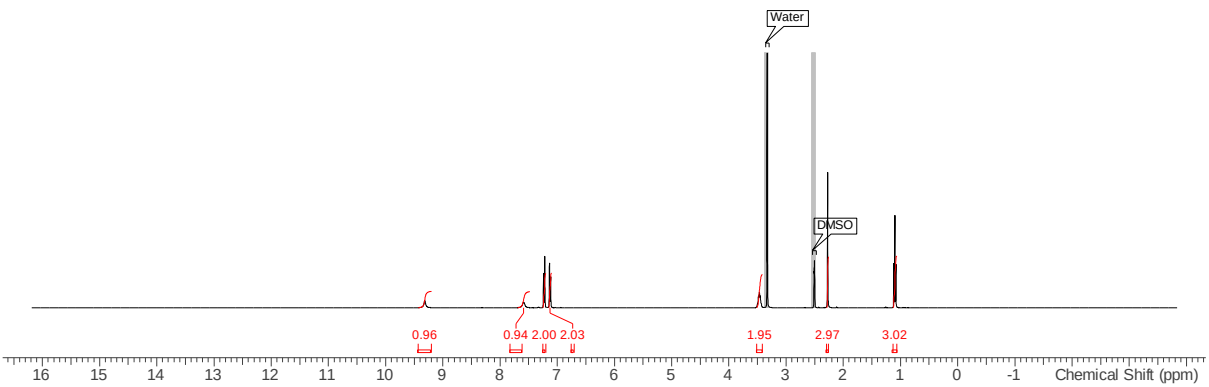


**Figure 3 -** $^{1}$H NMR (400 MHz, DMSO-$d_6$) spectrum of 1-(p-tolyl)-3-ethylthiourea.

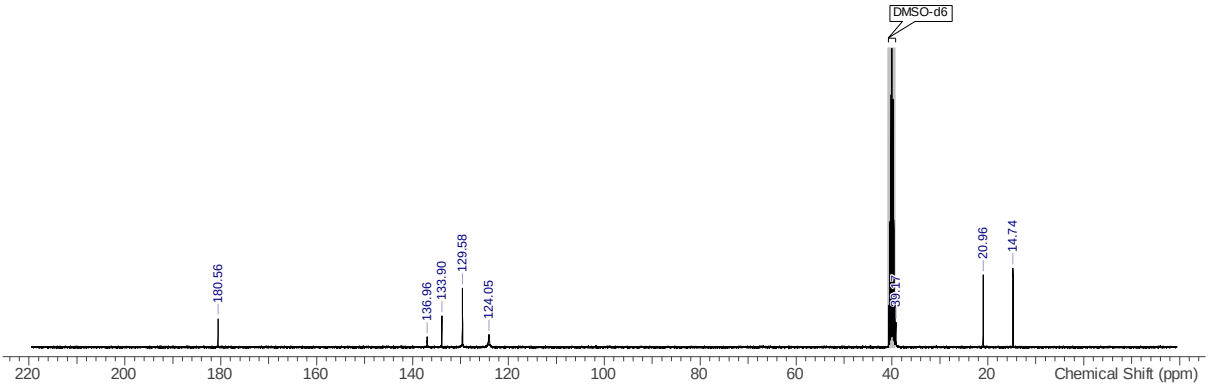


**Figure 4 -** $^{13}$C NMR (101 MHz, DMSO-$d_6$) spectrum of 1-(p-tolyl)-3-ethylthiourea.

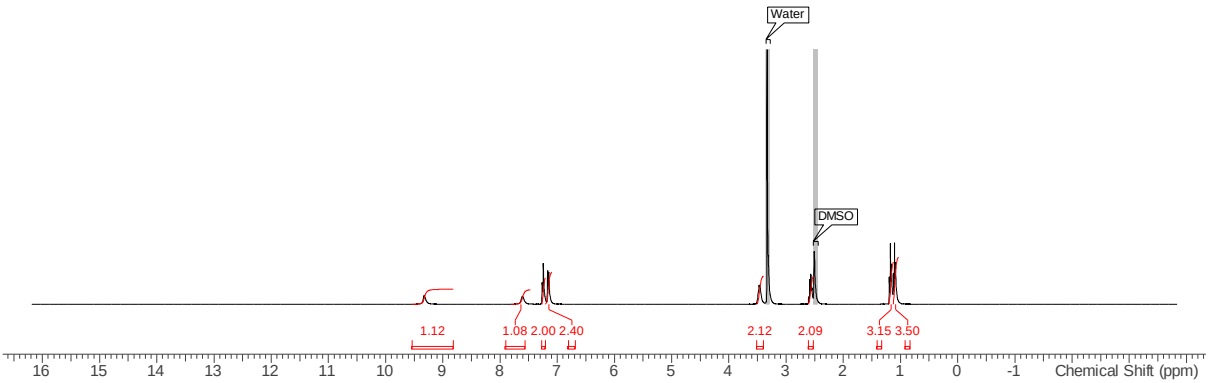


**Figure 5 -** $^{1}$H NMR (400 MHz, DMSO-$d_6$) spectrum of 1-(4-ethylphenyl)-3-ethylthiourea.

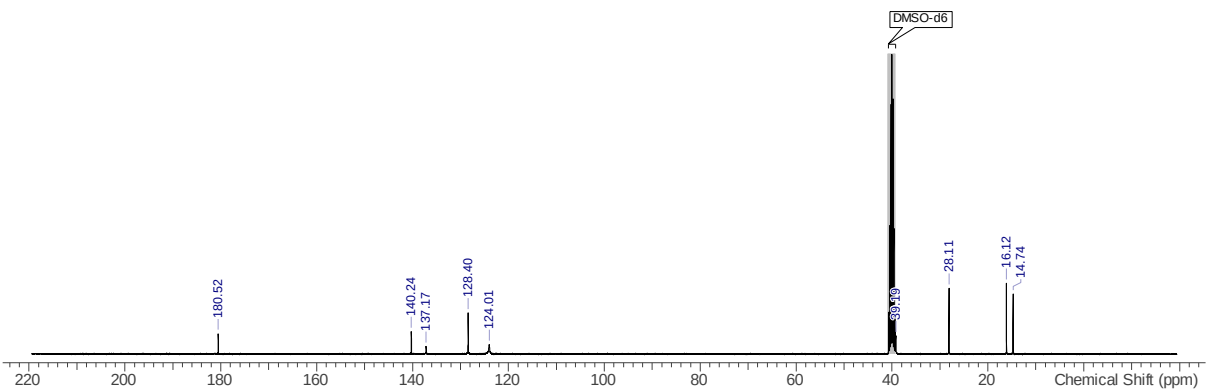


**Figure 6 -** $^{13}$C NMR (101 MHz, DMSO-$d_6$) spectrum of 1-(4-ethylphenyl)-3-ethylthiourea.

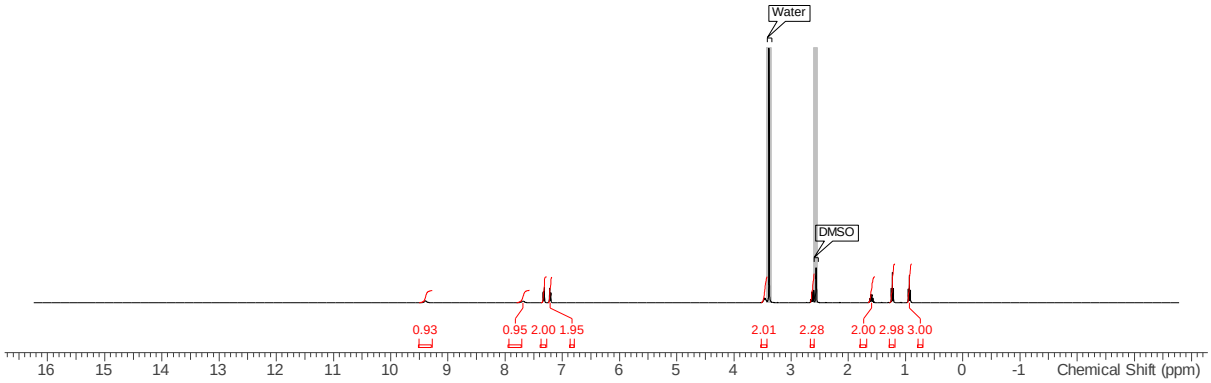


**Figure 7 -** $^{1}$H NMR (400 MHz, DMSO-$d_6$) spectrum of 1-(4-ethylphenyl)-3-propylthiourea.

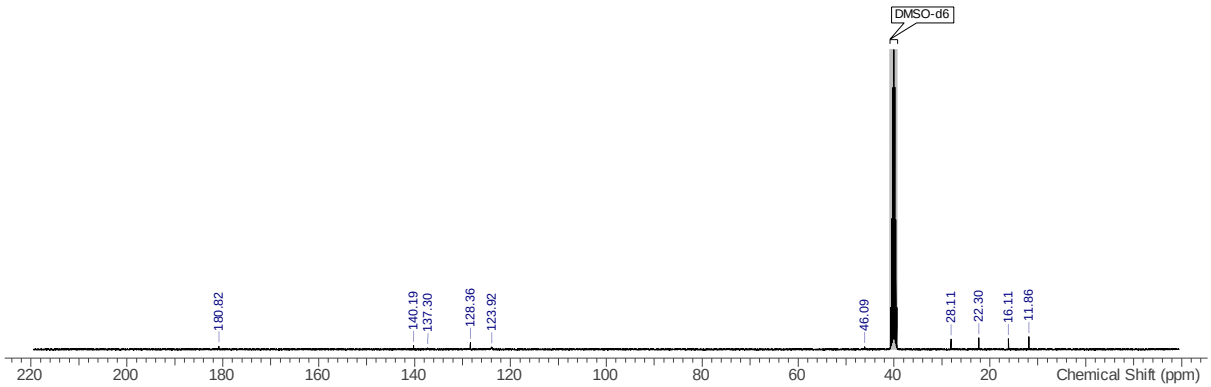


**Figure 8 -** $^{13}$C NMR (101 MHz, DMSO-$d_6$) spectrum of 1-(4-ethylphenyl)-3-propylthiourea.

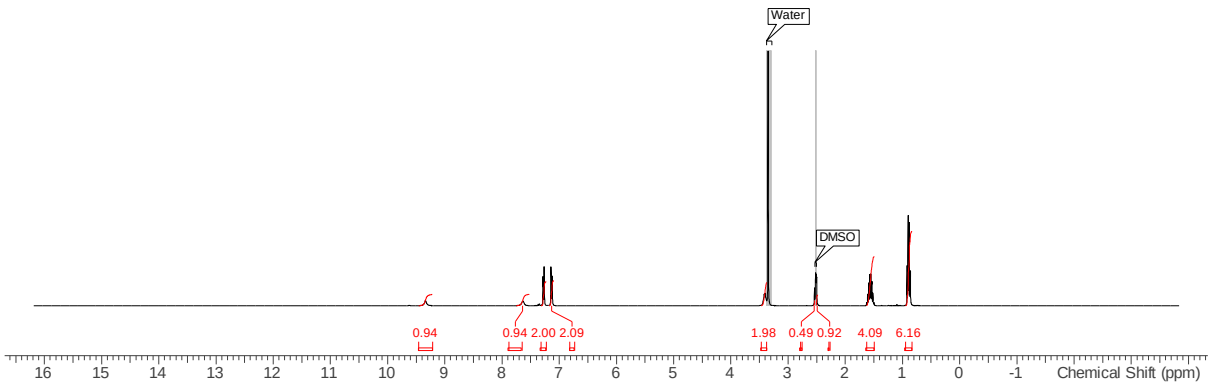


**Figure 9 -** $^{1}$H NMR (400 MHz, DMSO-$d_6$) spectrum of 1-(4-propylphenyl)-3-propylthiourea.

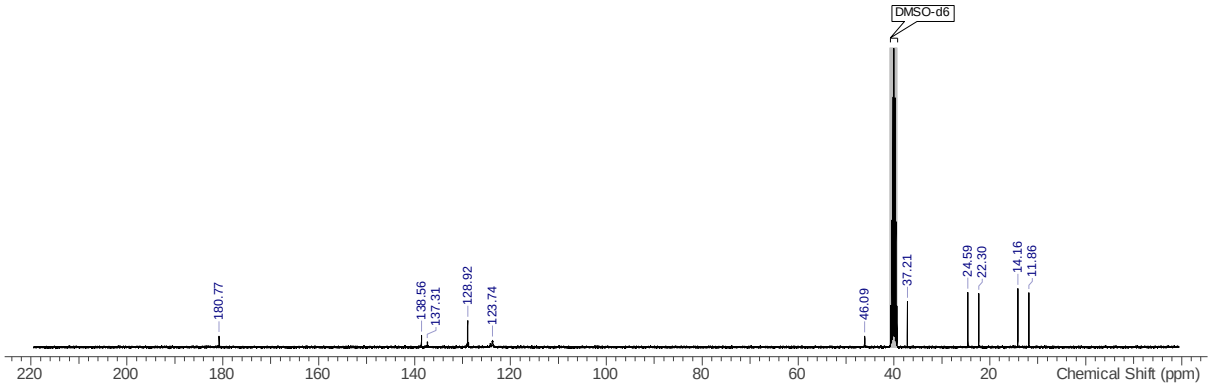


**Figure 10 -** $^{13}$C NMR (101 MHz, DMSO-$d_6$) spectrum of 1-(4-propylphenyl)-3-propylthiourea.

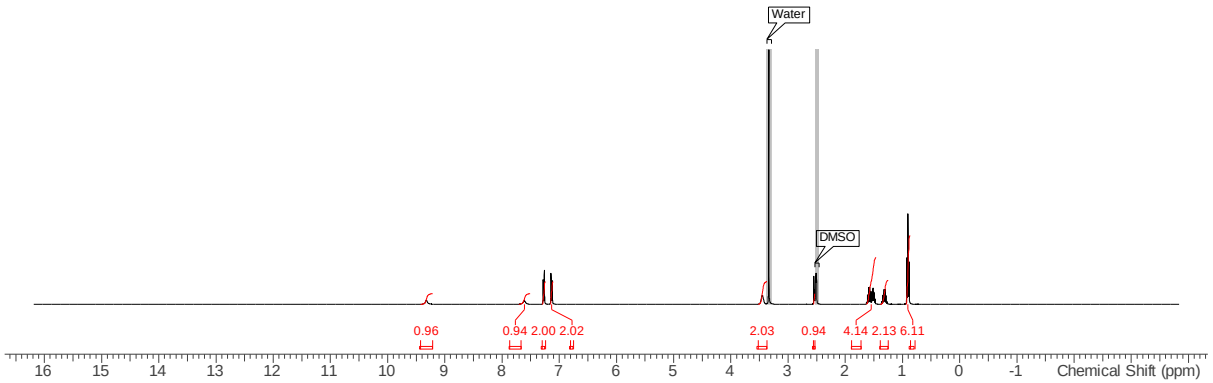


**Figure 11 -** $^{1}$H NMR (400 MHz, DMSO-$d_6$) spectrum of 1-(4-propylphenyl)-3-butylthiourea.

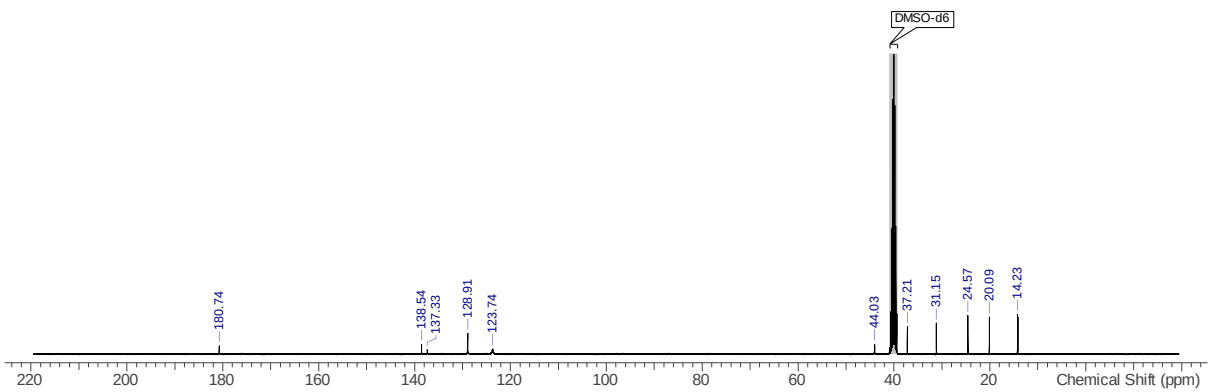


**Figure 12 -** $^{13}$C NMR (101 MHz, DMSO-$d_6$) spectrum of 1-(4-propylphenyl)-3-butylthiourea.

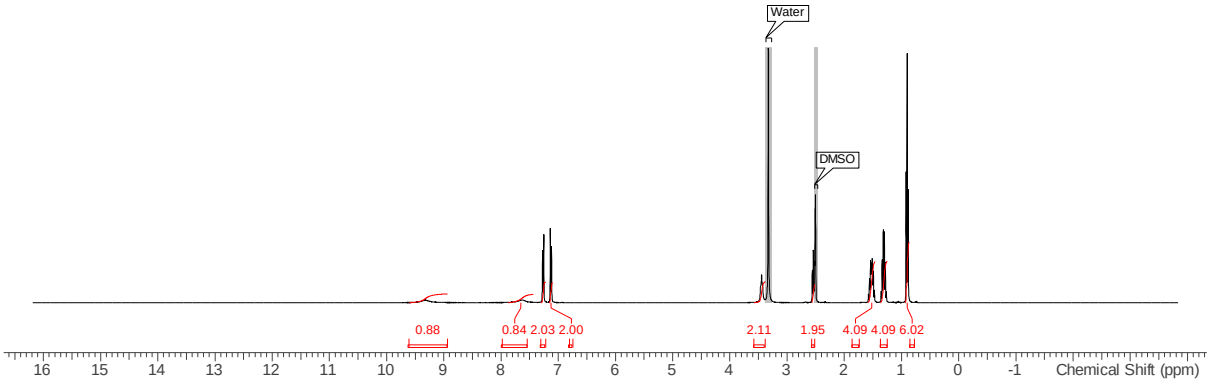


**Figure 13 -** $^{1}$H NMR (400 MHz, DMSO-$d_6$) spectrum of 1-(4-butylphenyl)-3-butylthiourea.

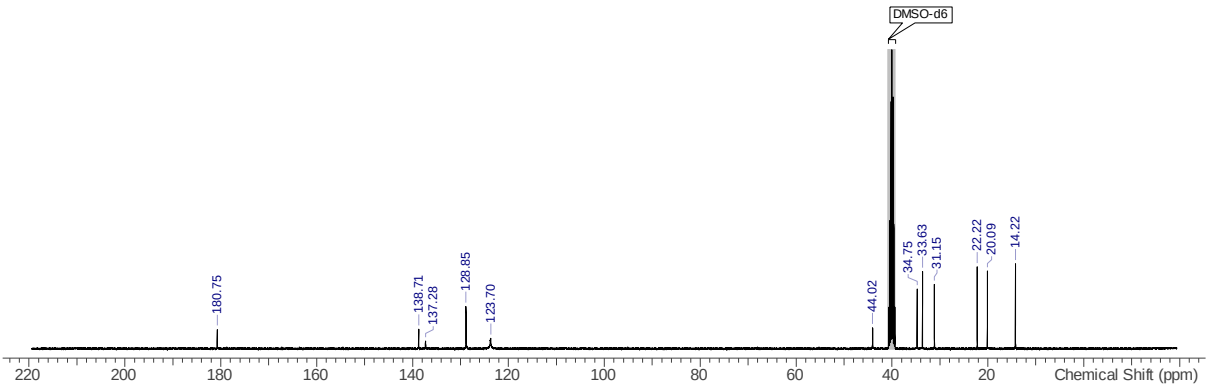


**Figure 14 -** $^{13}$C NMR (101 MHz, DMSO-$d_6$) spectrum of 1-(4-butylphenyl)-3-butylthiourea.

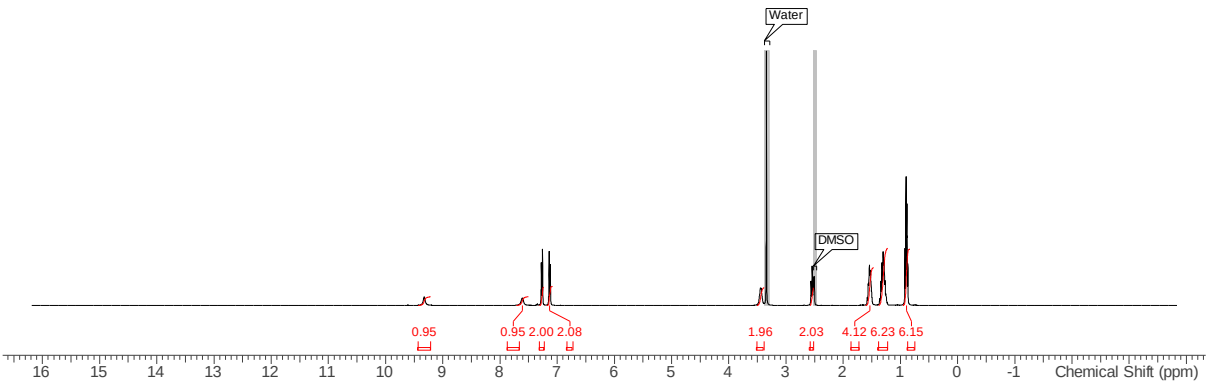


**Figure 15 -** $^{1}$H NMR (400 MHz, DMSO-$d_6$) spectrum of 1-(4-butylphenyl)-3-pentylthiourea.

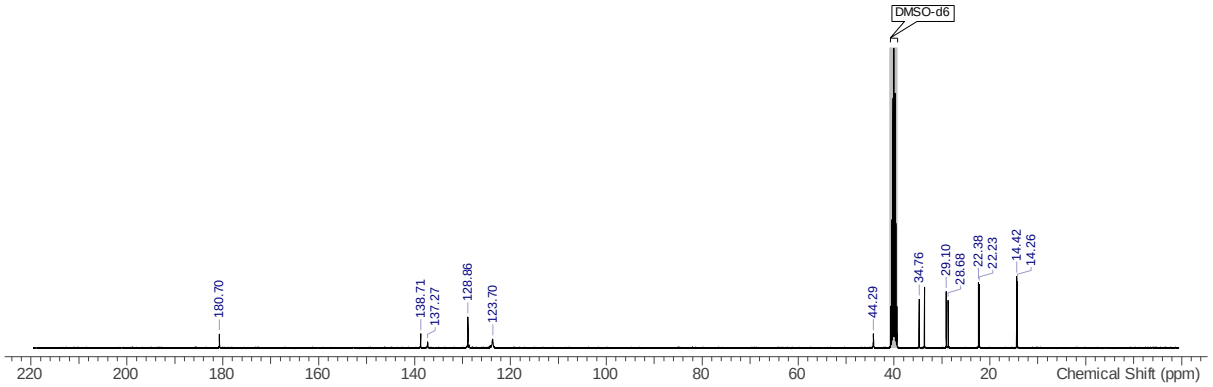


**Figure 16 -** $^{13}$C NMR (101 MHz, DMSO-$d_6$) spectrum of 1-(4-butylphenyl)-3-pentylthiourea.

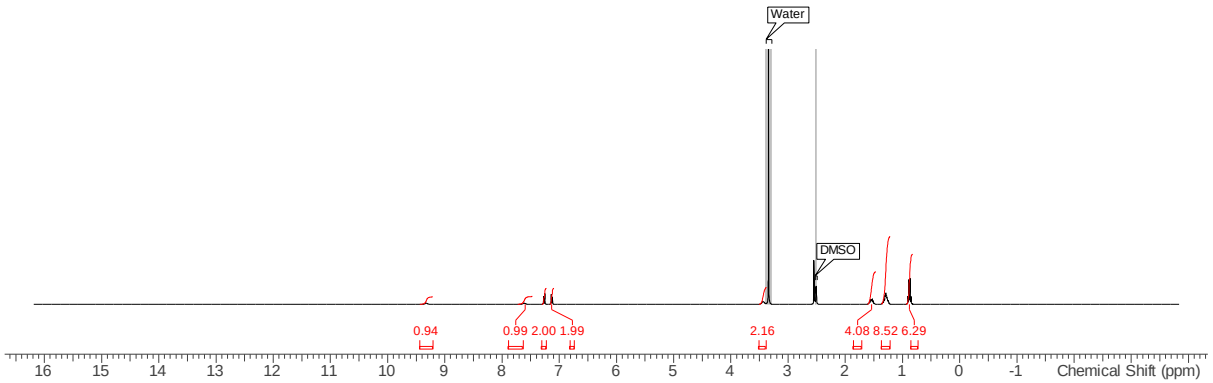


**Figure 17 -** $^{1}$H NMR (400 MHz, DMSO-$d_6$) spectrum of 1-(4-pentylphenyl)-3-pentylthiourea.

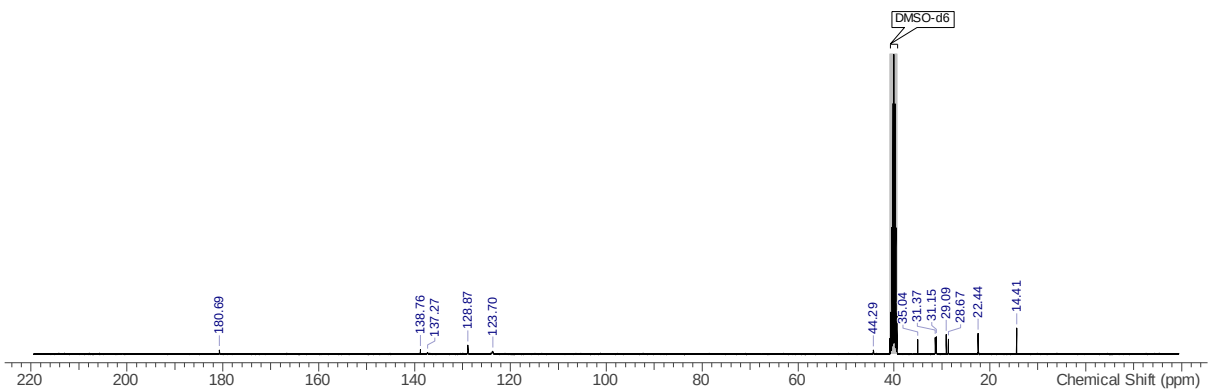


**Figure 18 -** $^{13}$C NMR (101 MHz, DMSO-$d_6$) spectrum of 1-(4-pentylphenyl)-3-pentylthiourea.

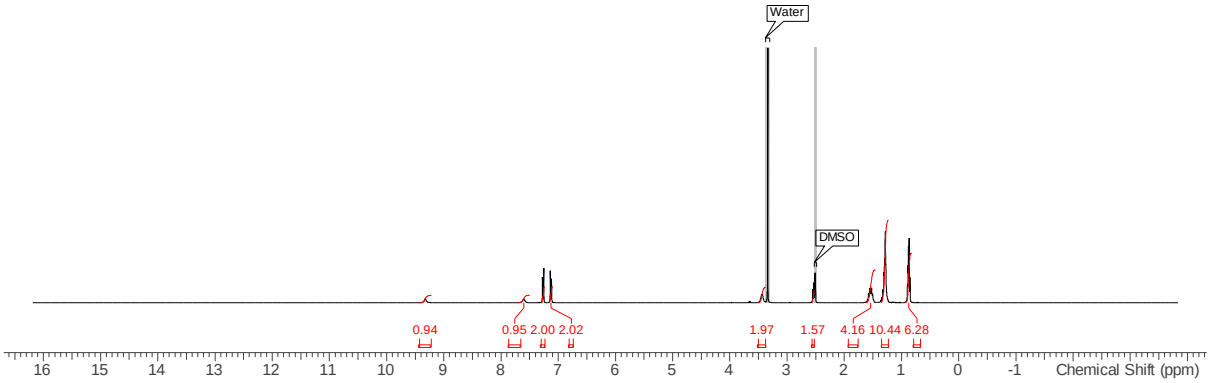


**Figure 19 -** $^{1}$H NMR (400 MHz, DMSO-$d_6$) spectrum of 1-(4-pentylphenyl)-3-hexylthiourea.

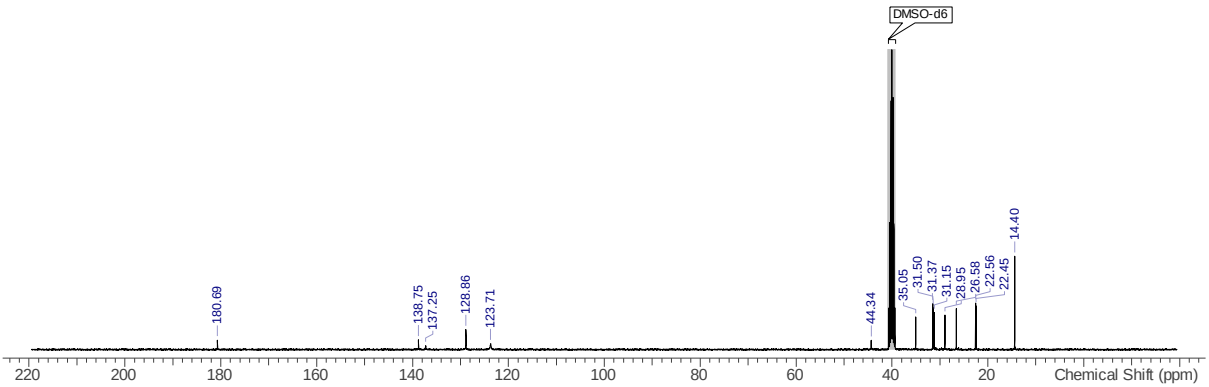


**Figure 20 -** $^{13}$C NMR (101 MHz, DMSO-$d_6$) spectrum of 1-(4-pentylphenyl)-3-hexylthiourea.

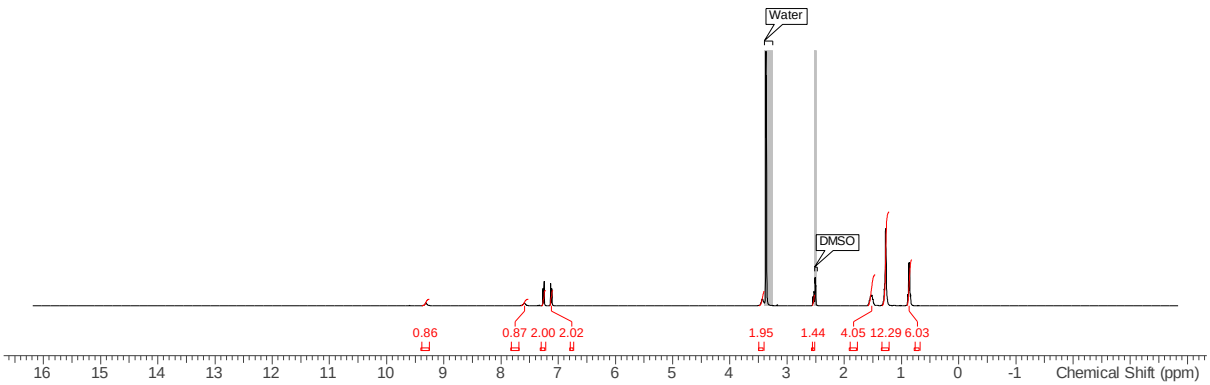


**Figure 21 -** $^{1}$H NMR (400 MHz, DMSO-$d_6$) spectrum of 1-(4-hexylphenyl)-3-hexylthiourea.

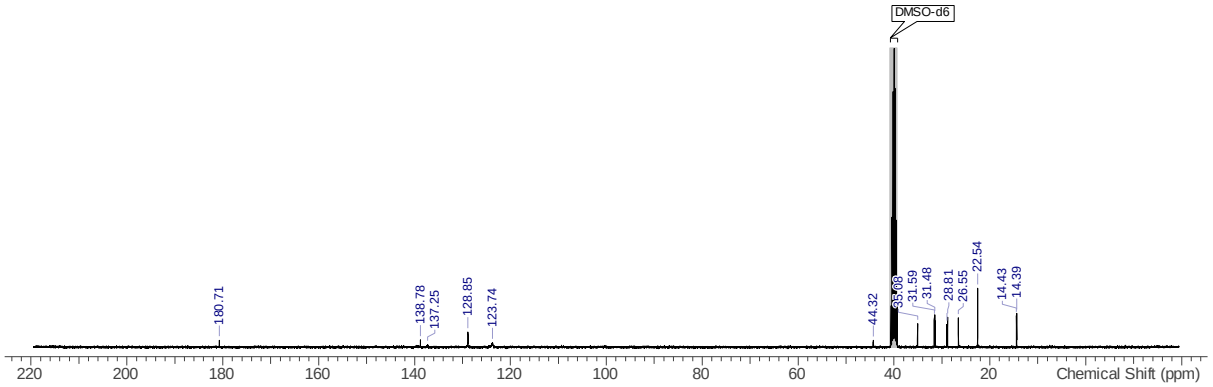


**Figure 22 -** $^{13}$C NMR (101 MHz, DMSO-$d_6$) spectrum of 1-(4-hexylphenyl)-3-hexylthiourea.

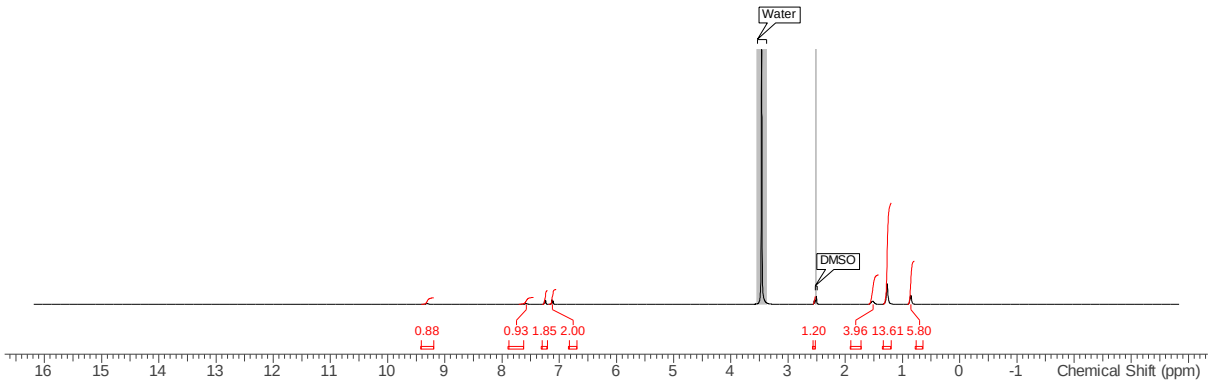


**Figure 23 -** $^{1}$H NMR (400 MHz, DMSO-$d_6$) spectrum of 1-(4-hexylphenyl)-3-heptylthiourea.

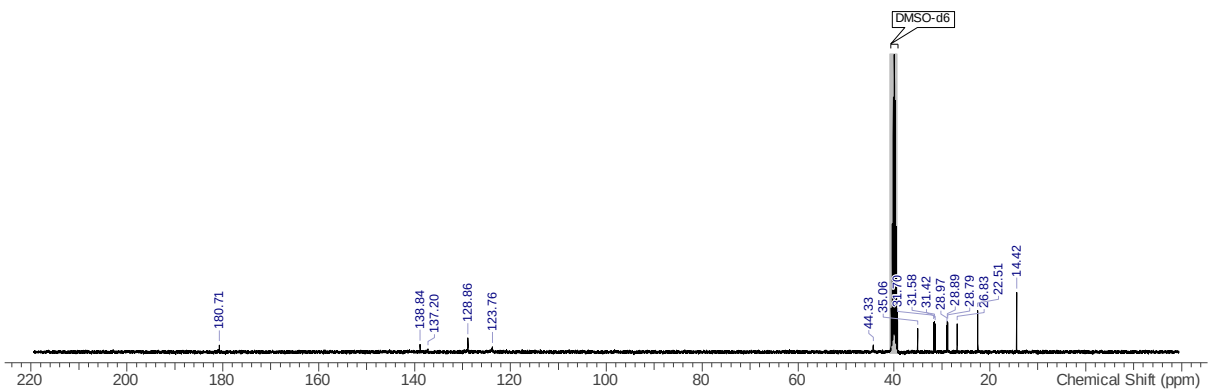


**Figure 24 -** $^{13}$C NMR (101 MHz, DMSO-$d_6$) spectrum of 1-(4-hexylphenyl)-3-heptylthiourea.

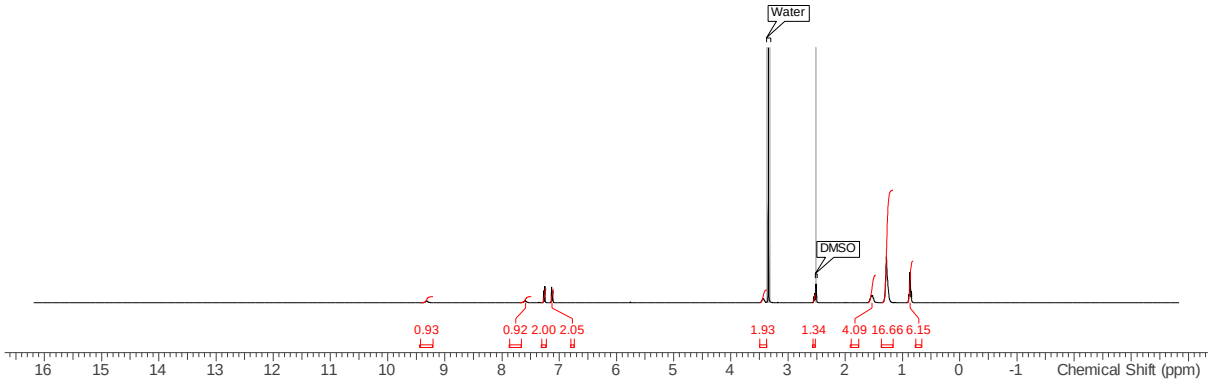


**Figure 25 -** $^{1}$H NMR (400 MHz, DMSO-$d_6$) spectrum of 1-(4-heptylphenyl)-3-heptylthiourea.

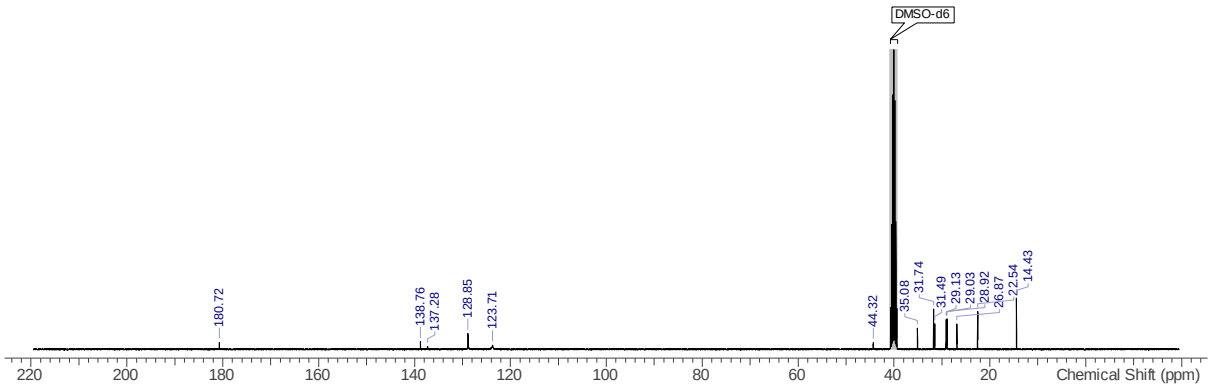


**Figure 26** - $^{13}$C NMR (101 MHz, DMSO-$d_6$) spectrum of 1-(4-heptylphenyl)-3-heptylthiourea.

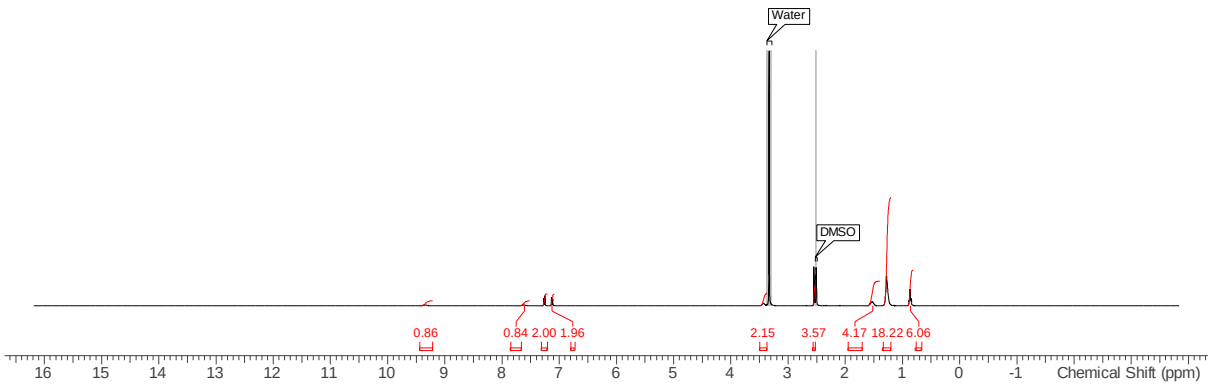


**Figure 27 -** $^{1}$H NMR (400 MHz, DMSO-$d_6$) spectrum of 1-(4-heptylphenyl)-3-octylthiourea.

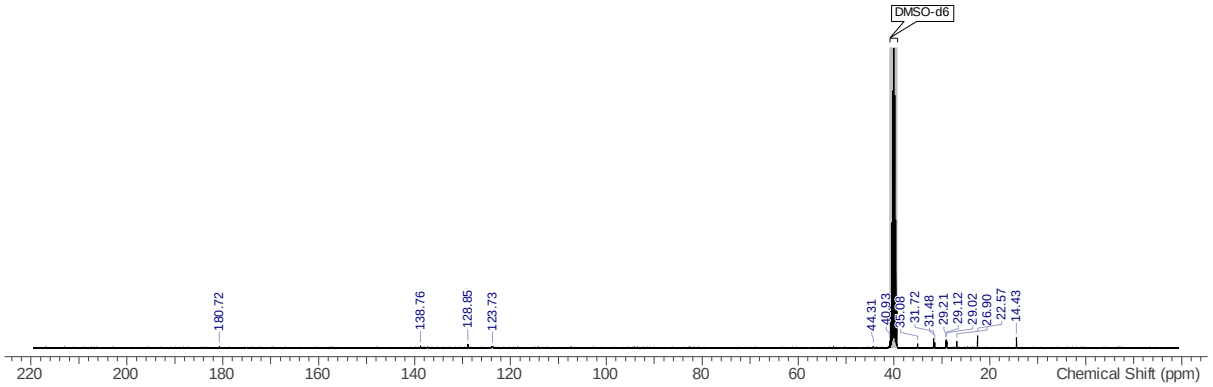


**Figure 28 -** $^{13}$C NMR (101 MHz, DMSO-$d_6$) spectrum of 1-(4-heptylphenyl)-3-octylthiourea.

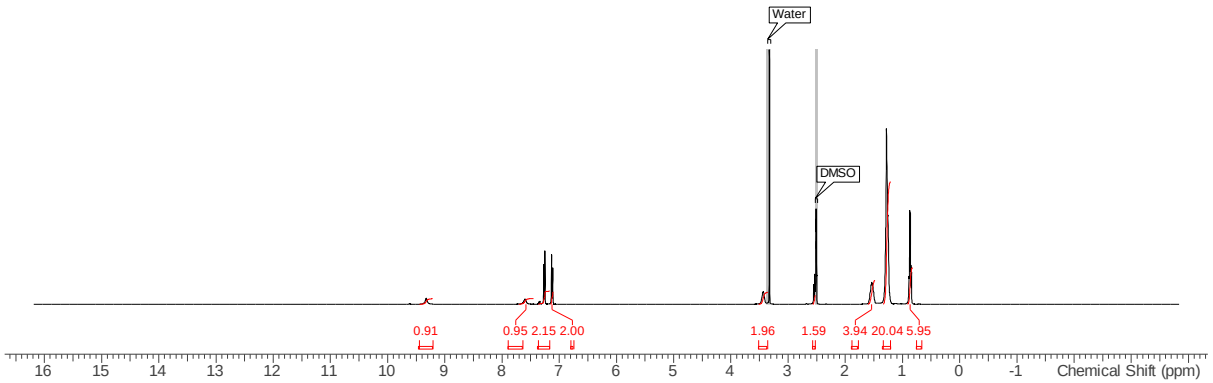


**Figure 29 -** $^{1}$H NMR (400 MHz, DMSO-$d_6$) spectrum of 1-(4-octylphenyl)-3-octylthiourea.

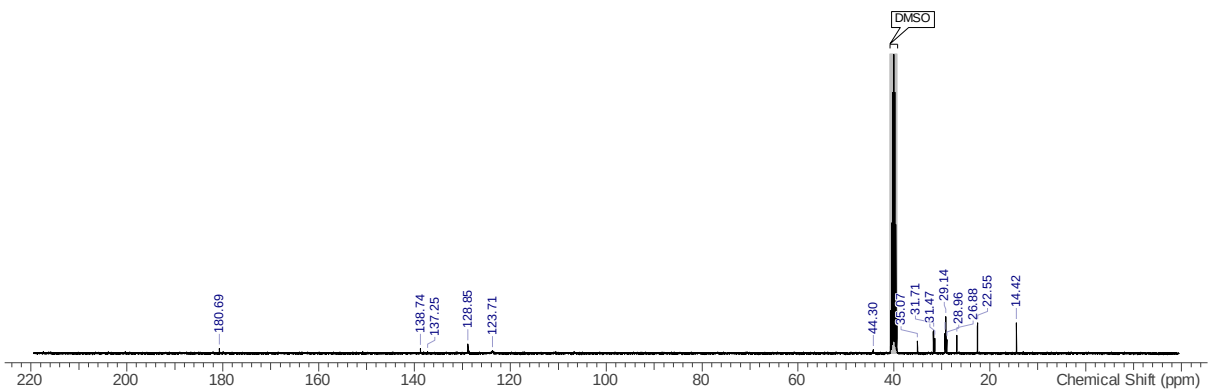


**Figure 30 -** $^{13}$C NMR (101 MHz, DMSO-$d_6$) spectrum of 1-(4-octylphenyl)-3-octylthiourea.

# 3 ClogP Calculations

The calculated log P values (P = octanol/water partition coefficient) for each compound were calculated using various methods, using open online calculation tools[4, 5] or algorithms built into common programs such as ACD/LogP and Chemdraw. The obtained values are listed in Table .

| # | RT /min | Chemdraw | VCCLab Consensus | ALOGPs | AClogP | ALOGP | MLOGP | KOWWIN | XLOGP2 | XLOGP3 | ACD/LogP |
|---|---|---|---|---|---|---|---|---|---|---|---|
| **1** | 0.27 | 1.41 | 1.81 | 1.50 | 2.11 | 2.19 | 1.95 | 1.91 | 1.59 | 1.42 | 1.42 |
| **2** | 0.30 | 1.91 | 2.19 | 1.74 | 2.42 | 2.68 | 2.25 | 2.46 | 2.03 | 1.78 | 1.88 |
| **3** | 0.35 | 2.44 | 2.65 | 2.45 | 2.78 | 3.14 | 2.54 | 2.95 | 2.49 | 2.22 | 2.41 |
| **4** | 0.41 | 2.97 | 3.16 | 2.87 | 3.24 | 3.66 | 2.82 | 3.44 | 2.85 | 3.22 | 2.94 |
| **5** | 0.52 | 3.50 | 3.62 | 3.33 | 3.71 | 4.12 | 3.09 | 3.93 | 3.42 | 3.76 | 3.47 |
| **6** | 0.68 | 4.03 | 4.07 | 3.86 | 4.17 | 4.57 | 3.36 | 4.42 | 3.99 | 4.12 | 4.01 |
| **7** | 0.93 | 4.55 | 4.54 | 4.37 | 4.64 | 5.03 | 3.61 | 4.91 | 4.56 | 4.66 | 4.54 |
| **8** | 1.28 | 5.08 | 4.99 | 4.77 | 5.10 | 5.49 | 3.86 | 5.40 | 5.12 | 5.20 | 5.07 |
| **9** | 1.85 | 5.61 | 5.45 | 5.20 | 5.57 | 5.94 | 4.11 | 5.89 | 5.69 | 5.74 | 5.60 |
| **10** | 2.67 | 6.14 | 5.91 | 5.71 | 6.03 | 6.40 | 4.34 | 6.38 | 6.26 | 6.28 | 6.13 |
| **11** | 3.99 | 6.67 | 6.38 | 6.20 | 6.49 | 6.85 | 4.57 | 6.88 | 6.83 | 6.82 | 6.66 |
| **12** | 5.91 | 7.20 | 6.70 | 6.74 | 6.96 | 7.31 | 4.80 | 7.37 | 6.35 | 7.37 | 7.19 |
| **13** | 8.93 | 7.73 | 7.25 | 7.15 | 7.42 | 7.77 | 5.94 | 7.86 | 6.70 | 7.91 | 7.72 |
| **14** | 13.44 | 8.26 | 7.69 | 7.52 | 7.89 | 8.22 | 6.16 | 8.35 | 7.27 | 8.45 | 8.26 |
| **15** | 20.55 | 8.79 | 8.10 | 7.87 | 8.35 | 8.68 | 6.37 | 8.84 | 7.63 | 8.99 | 8.79 |

**Table 1–** Clog P values and isocratic RP-HPLC retention times for compounds

Each method was evaluated by studying quality of the correlation of the retention factor on a C18 RP-HPLC column with the Clog P values. Compounds were eluted isocratically over 30 minutes with 60% acetonitrile/water. The retention factor k' is calculated from the retention time (RT) of each compound and the column dead time (the time taken for an unretained compound to pass through the column, $t_0$).

$$k' = \frac{RT - t_0}{t_0}$$

The dead time ($t_0$) of the column was determined by comparison of the relative retention times of the compounds. As the series is homologous, plotting the RT($n_c$) (retention time, number of carbons = n) against RT($n_{c+1}$) gives a straight line allowing $t_0$ to be calculated as follows[6] in Figure 31. The retention time values from the RP-HPLC are given in Table 1.

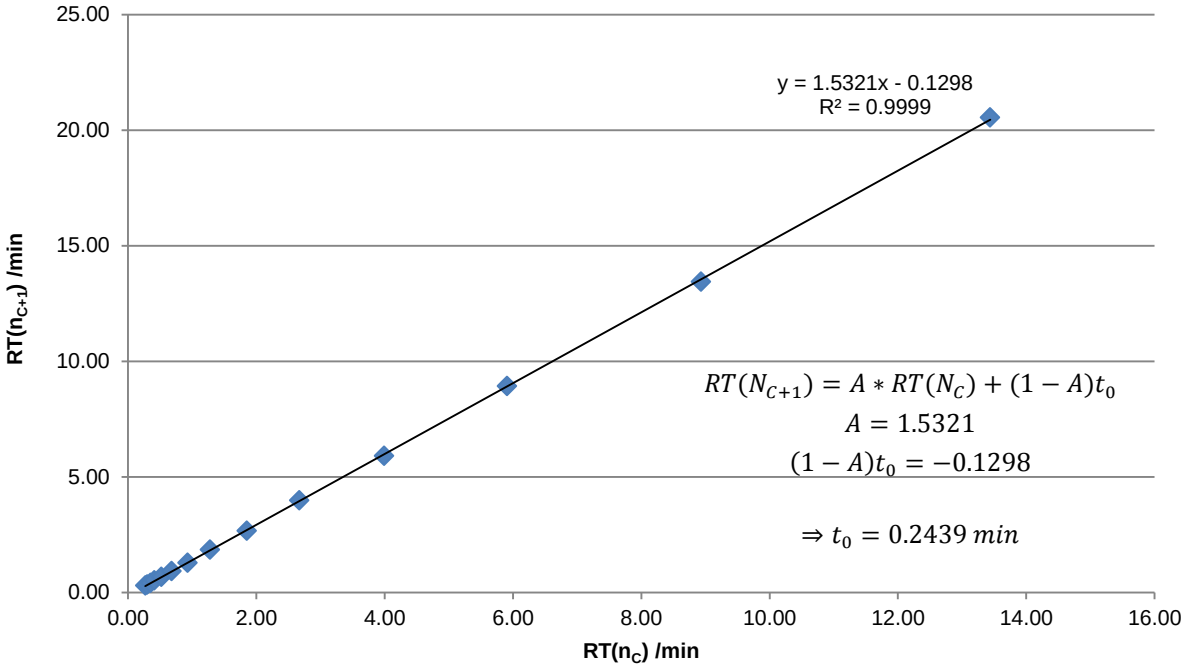


**Figure 31 –** Determining $t_0$ for the RP-HPLC experiments. Retention times plot plus calculation steps. Method adapted from [6].

With $t_0$ = 0.2439 min, k' could be calculated for each compound. As log k' from isocratic HPLC data correlates linearly with log P[6, 7], the values were plotted against the Clog P values from the tested calculation methods.

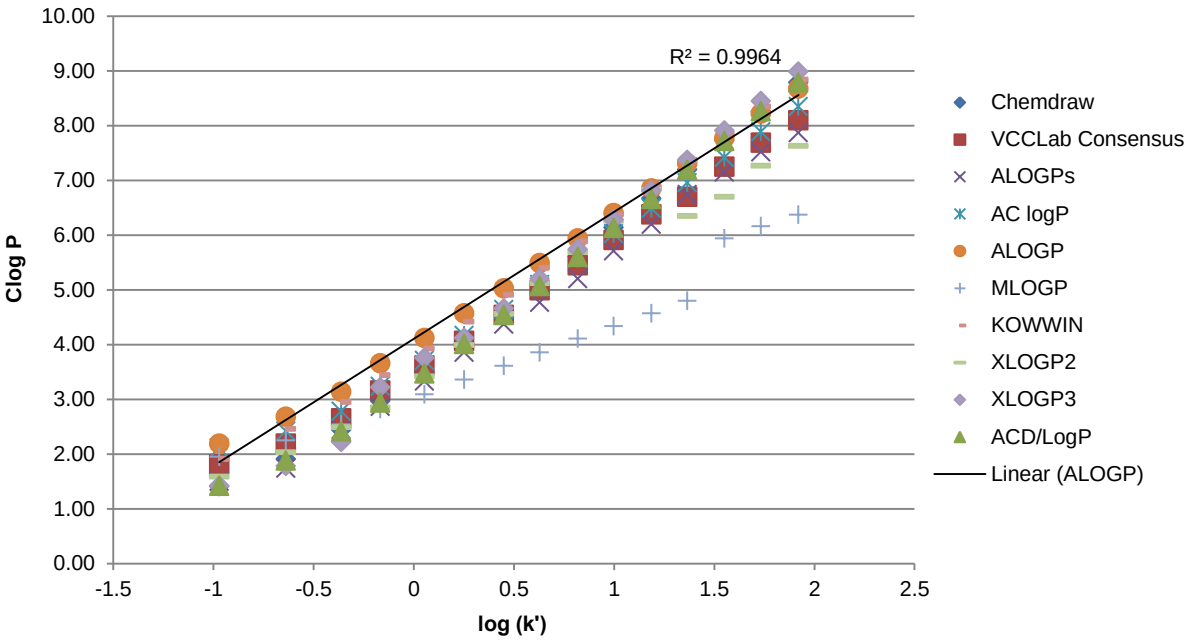


**Figure 32 –** Plot of log (k') against calculated log P from various computational methods. Black line represents the linear fit of the data from the ALOGP model, with the correlation coefficient.

Although several methods gave very strong correlations, the ALOGP model (Ghose-Crippen) was chosen as it gave the highest correlation coefficient ($R^2 = 0.9964$).

# 4 Transport Studies Experimental

## 4.1 Mixed Vesicle Synthesis for $Cl^-/NO3^-$ Transport Assays

POPC, POPG, POPE and DPPC were all purchased from Avanti Polar Lipids, Cholesterol from Sigma-Aldrich. POPG, POPE and CHOL were used as supplied; POPC was stored as a solution in chloroform (1 g lipid in 35 ml). Internal buffer was prepared containing 489 mM NaCl and 5 mM phosphate buffers, external buffer was prepared containing 489 mM $NaNO_3$ and 5mM phosphate buffers. Both buffers were adjusted to pH 7.2.

POPC solution was added to a 50 ml RBF of known mass and the solvent removed under reduced pressure forming a film of dried lipid. The film was dried *in vacuo* for at least 4 hours and the mass of lipid weighed. For mixed vesicles, the correct mass of the second lipid to achieve the correct molar ratio was then weighed out, dissolved in chloroform and the solution transferred in a quantitative manner to the RBF, the POPC film re-dissolving in this solution. The solvent was again removed under reduced pressure and the film dried for at least 4 hours as before.

The dry lipid was re-suspended in a known quantity of internal buffer (about 4 ml per 120 mg lipid). This suspension was subjected to 9 freeze-thaw cycles in liquid nitrogen before being allowed to rest for 30 minutes. The suspension was extruded 25 times through a 200 nm polycarbonate membrane. The volume of suspension recovered after extrusion was measured before dialysing overnight against ~1.8 l external buffer. The vesicle suspension was finally diluted to 10 ml in external buffer to obtain a solution of known concentration (adjusted for solution loss during extrusion).

## 4.2 $Cl^-/NO_3^-$ Transport Assays

For each trial, a sample of dialysed vesicles was suspending in external buffer to a concentration of 1 mM (total volume 5 ml). The sample was equipped with a stirrer bar and Accumet chloride selective electrode. The electrode was connected to a Thermo Scientific Orion Star A321 Portable pH Meter linked to Thermo Star Com data logging software. Transport assays were initiated by the addition of a 10 mM solution in DMSO of the compound to be tested, such that loading of transporter was 1 % with respect to lipid.

The electrode voltage was recorded every 3 s for 5 minutes before addition of a detergent solution (polyoxyethylene-(8)-lauryl ether, TCI, 1 g in 8 ml 7:1 $H_2O$:DMSO, 50 µl) to lyse the vesicles. The final reading was taken at 7 minutes and the value at this time taken as 100 % efflux. For each concentration of transporter, trials were conducted in triplicate and averaged and the mV readings from the electrode were converted to a % $Cl^-$ efflux after calibration with NaCl solutions of known concentration.

Attempts to fit the trial curves to various sigmoidal/exponential/growth/decay functions yielded unsatisfactory results. Errors on calculated values were large, especially for compounds at either end of the series. Thus to obtain values for the initial rate, an approach similar to that used by Quesada et al.[8] was used to quantify the initial rate. The data points for the first 30 seconds of each run were considered to be approximately linear and the rate taken as the gradient obtained by performing a linear regression on the data. $r^2$ values for the regression analysis were always greater than 0.88, with the majority of values (ie those not at the extremes of lipophilicity) in excess of 0.94.

## 4.3 $SO_4^{2-}$ / $NO_3^-$ Spike Assays

Mixed vesicles were prepared as per section 4.1, with the external buffer containing 162 mM $NaSO_4$ and 5 mM phosphate buffers, adjusted to pH 7.2. Assays were run in the same manner as the chloride/nitrate assays, with initiation of the experiment by addition of a 10mM solution in DMSO of the compound of interest. After 2 minutes, transport was initiated by the addition of a solution of

$NaNO_3$ such that the final concentration of nitrate was 40 mM. Detergent was added at 7 minutes and final reading taken at 9 minutes. The initial rate at 120 s was calculated by linear approximation as before.

## 4.4 Calcein Leakage Assays

A lipid film of 3:1 POPE:POPC was suspended in a solution of 100 mM calcein, 450 mM NaCl and 20 mM phosphate buffers (adjusted to pH 7.2). The suspension was freeze-thawed 9 times before aging for 30 minutes. The aged vesicles were then extruded 25 times through a 200 nm polycarbonate membrane. The un-encapsulated calcein was removed by size exclusion chromatography on a Sephadex G-50 using an $NaSO_4$ (162 mM, 20 mM phosphate buffers, adjusted to pH 7.2) solution as the eluent.

10 mM samples of compounds **1**, **7** and **15** were added to 1 mM samples of vesicles suspended in $NaSO_4$ solution (such that final loading was 1% wrt. lipid) and the fluorescence emission at 520 nm (after excitation at 490 nm) monitored for 16 hours using an Agilent Technologies Carey Eclipse Fluorescence Spectrophotometer. At the end of the experiment, the vesicles were lysed with detergent (polyoxyethylene-(8)-lauryl ether, TCI, 1 g in 8 ml 7:1 $H_2O$:DMSO, 50 µl) to calibrate for total calcein release. The fraction calcein release was calculated as follows:

$$Fraction\ Calecin\ release = \frac{I_t - I_0}{I_{FINAL} - I_0}$$

## 4.5 HPTS Internal pH Assays

A lipid film of 3:1 POPE:POPC was suspended in a solution of 1 mM HPTS, 489 mM NaCl and 5 mM phosphate buffers (adjusted to pH 7.2). The suspension was freeze-thawed 9 times before aging for 30 minutes. The aged vesicles were then extruded 25 times through a 200 nm polycarbonate membrane. The un-encapsulated HPTS was removed by size exclusion chromatography on a Sephadex G-50 using an $NaSO_4$ (162 mM, 5 mM phosphate buffers, adjusted to pH 7.2) solution as the eluent.

10 mM samples of the compound to be tested were added to 1 mM samples of vesicles suspended in $NaSO_4$ solution (such that final loading was 1% wrt. lipid), to commence a trial. The fluorescence emission at 510 nm after excitation at 403 and 460 nm was monitored for 5 minutes using an Agilent Technologies Carey Eclipse Fluorescence Spectrophotometer. At the end of the experiment, the vesicles were lysed with detergent (polyoxyethylene-(8)-lauryl ether, TCI, 1 g in 8 ml 7:1 $H_2O$:DMSO, 50 µl). The difference in emission intensity after excitation at 403 nm and 460 nm was converted to the internal pH of the vesicles using the following equation[9]:

$$pH = -\frac{1}{1.796}\ln\left(\frac{4.2055}{\frac{I_{460}}{I_{403}} - 1}\right)$$

## 4.6 Lucigenin Assays

A lipid film of 3:1 POPE:POPC was suspended in a solution of 2 mM lucigenin, 100 mM NaCl and 20 mM phosphate buffers (adjusted to pH 7.2). The suspension was freeze-thawed 9 times before aging for 30 minutes. The aged vesicles were then extruded 25 times through a 200 nm polycarbonate membrane. The un-encapsulated calcein was removed by size exclusion chromatography on a Sephadex G-50 using a NaCl (100 mM, 20 mM phosphate buffers, adjusted to pH 7.2) solution as the eluent.

The fluorescence emission at 520 nm (after excitation at 490 nm) 1 mM samples of vesicles suspended in NaCl solution was monitored using an Agilent Technologies Carey Eclipse Fluorescence Spectrophotometer. After 30 s, a solution of anion (1 M NaCl / 1M $NaNO_3$ / 0.5M $NaSO_4$) was added to the sample to a final concentration of 40mM. At 90 s, a 10 mM solution of the test compound in DMSO was added such that final loading was 1% wrt. lipid. After 390 s, the vesicles were lysed with detergent (polyoxyethylene-(8)-lauryl ether, TCI, 1 g in 8 ml 7:1 $H_2O$:DMSO, 50 µl).

# 5 Transport Studies Data

## 5.1 Transport Curves

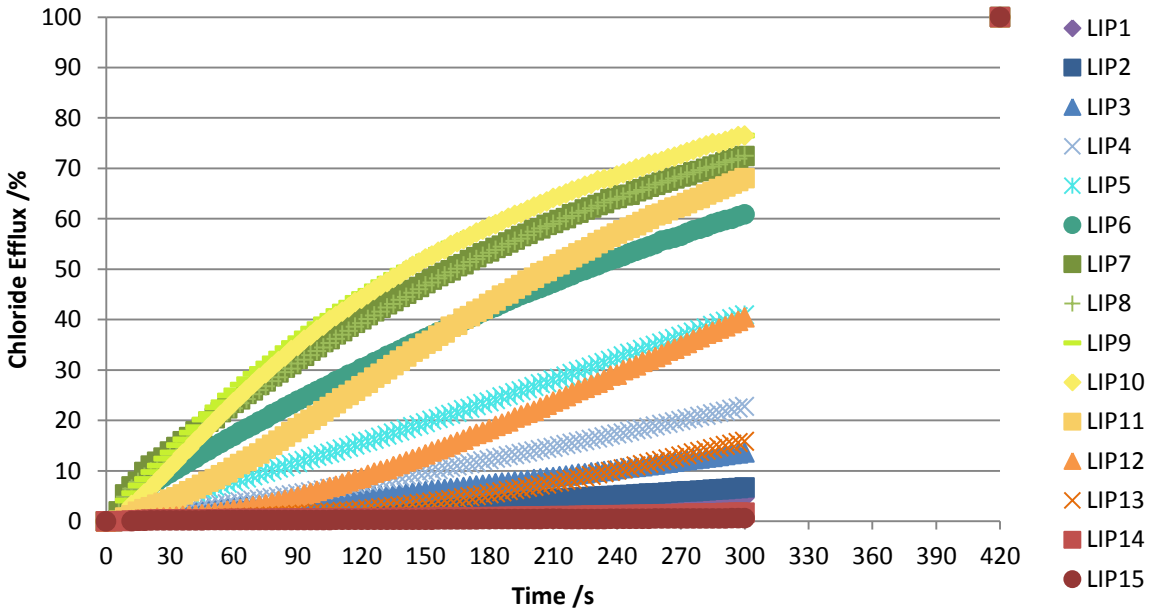


**Figure 33 –** Transport curves for compounds 1-15 in $Cl^-/NO_3^-$ assays in 100% POPC vesicles. Each curve represents the average of 3 trials.

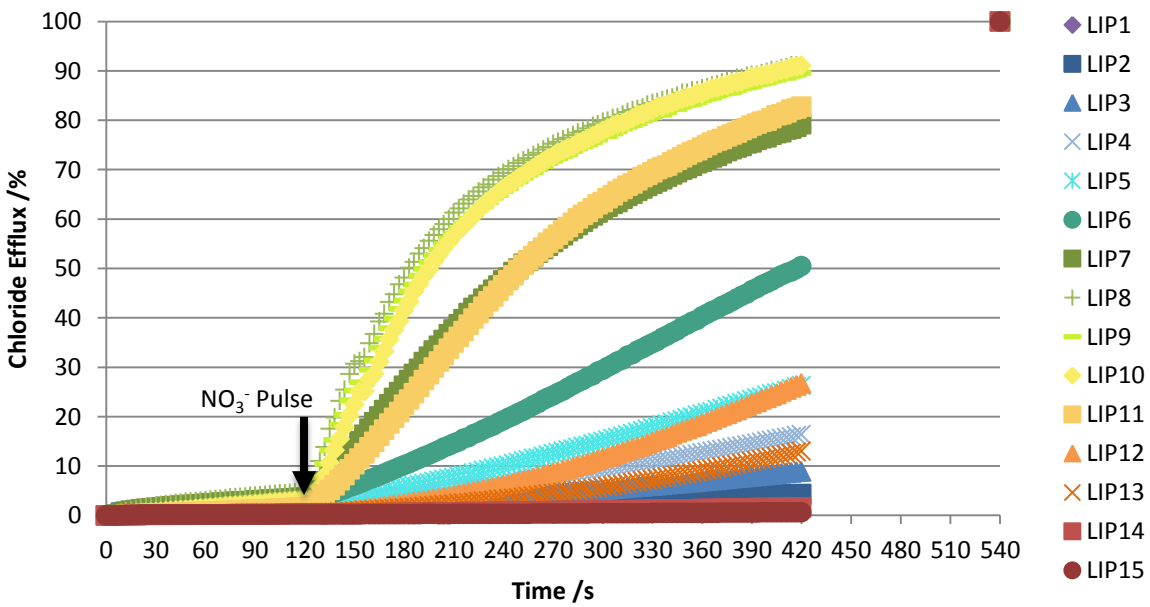


**Figure 34 –** Transport curves for compounds 1-15 in $SO_4^{2-}$ / $NO_3^-$ spike assays in 100% POPC vesicles. Each curve represents the average of 3 trials.

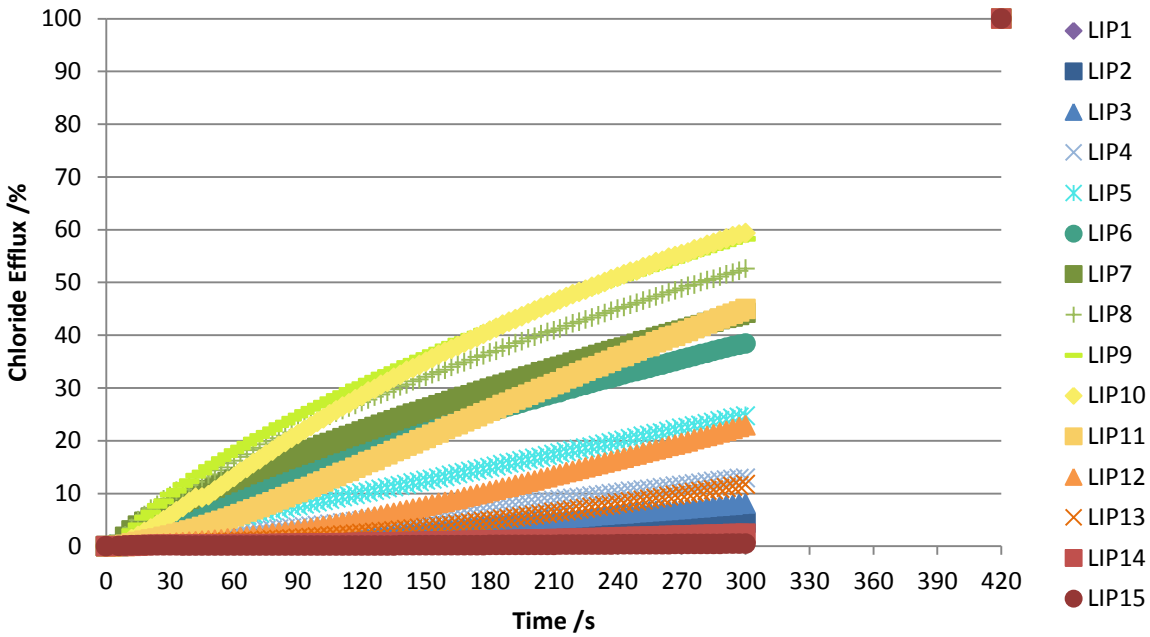


**Figure 35 –** Transport curves for compounds 1-15 in $Cl^-/NO_3^-$ assays in 100% POPG vesicles. Each curve represents the average of 3 trials.

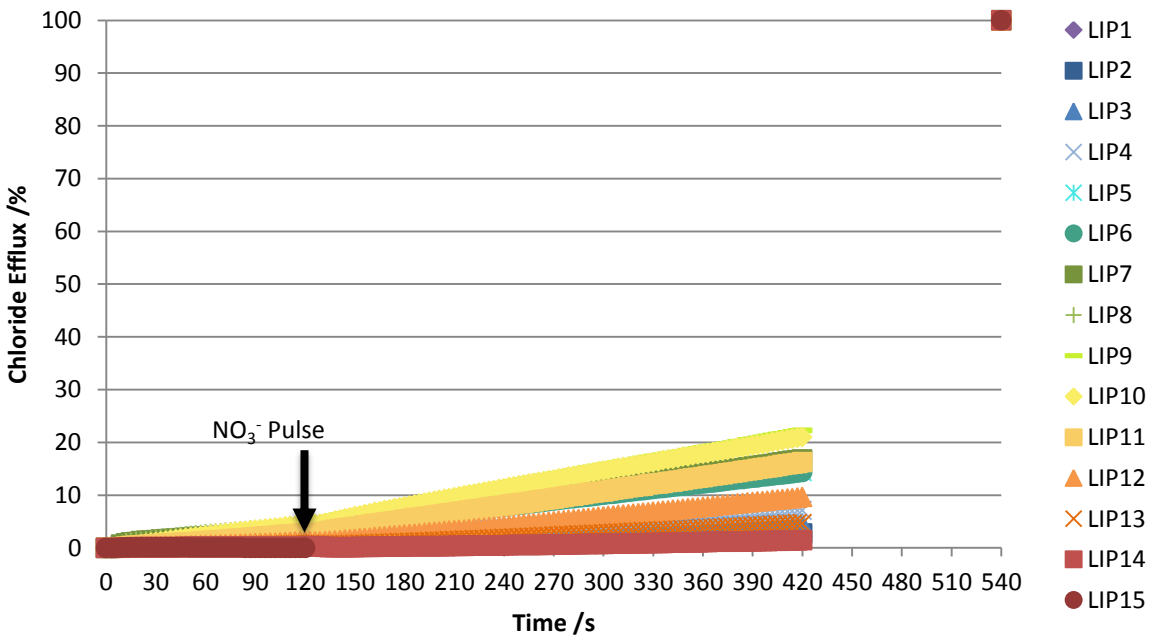


**Figure 36 –** Transport curves for compounds 1-15 in $SO_4^{2-}$ / $NO_3^-$ spike assays in 100% POPG vesicles. Each curve represents the average of 3 trials.

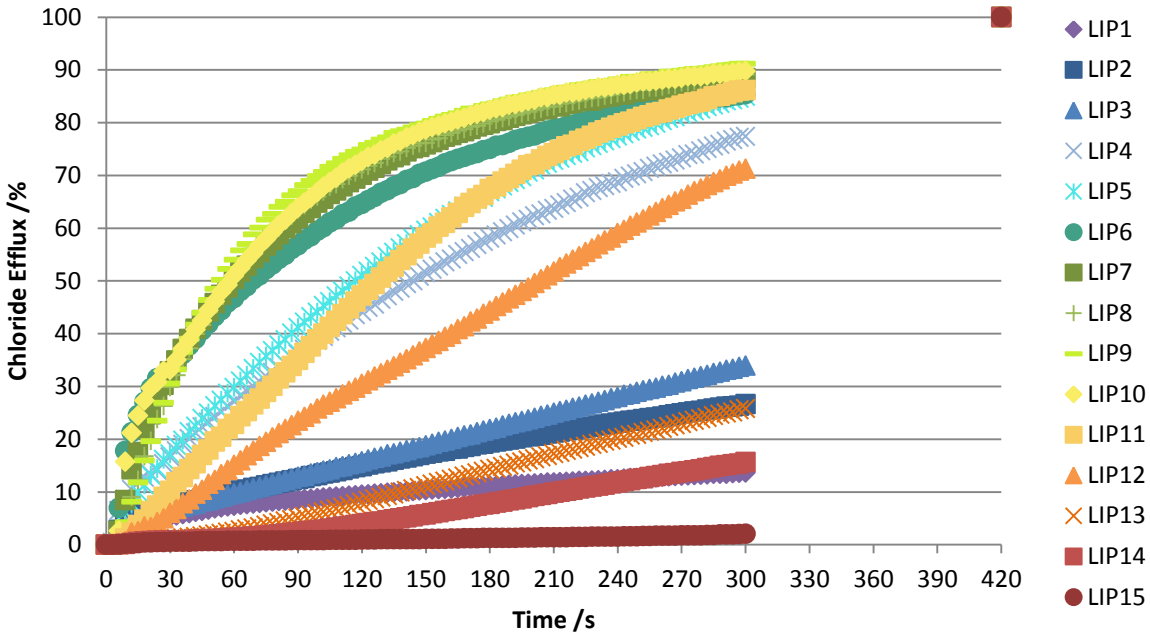


**Figure 37 –** Transport curves for compounds 1-15 in $Cl^-/NO_3^-$ assays in 3:1 POPE:POPC vesicles. Each curve represents the average of 3 trials.

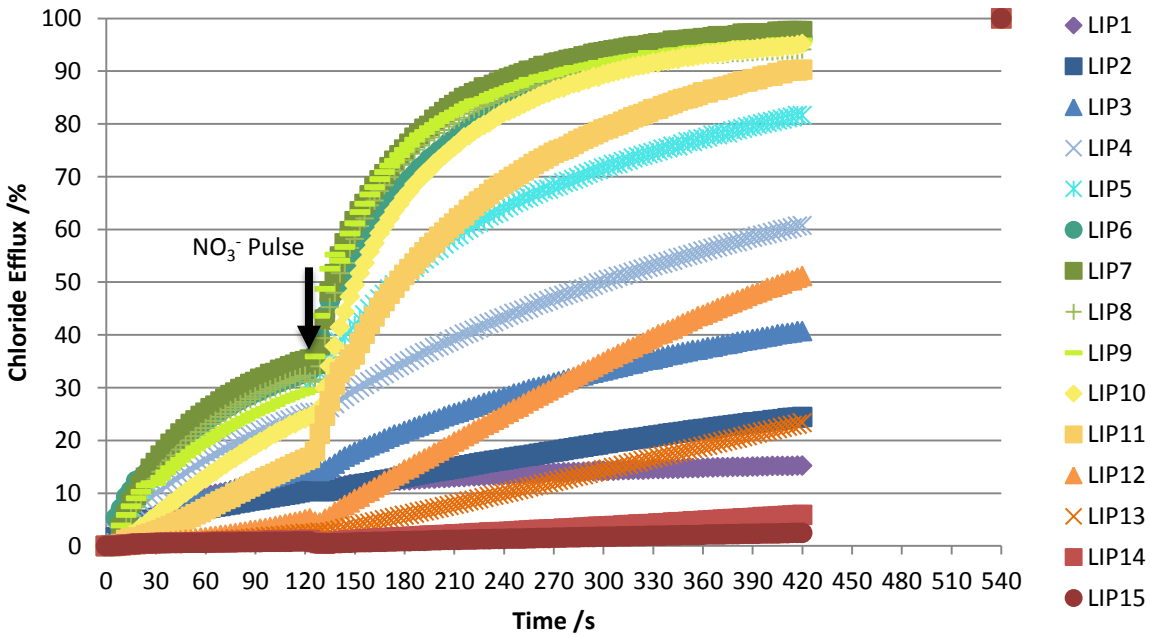


**Figure 38 -** Transport curves for compounds 1-15 in $SO_4^{2-}$ / $NO_3^-$ spike assays in 3:1 POPE:POPC vesicles. Each curve represents the average of 3 trials. Possible sulfate transport before the addition of nitrate is observed before the addition of nitrate. Mechanisms for this are investigated in section 5.2.

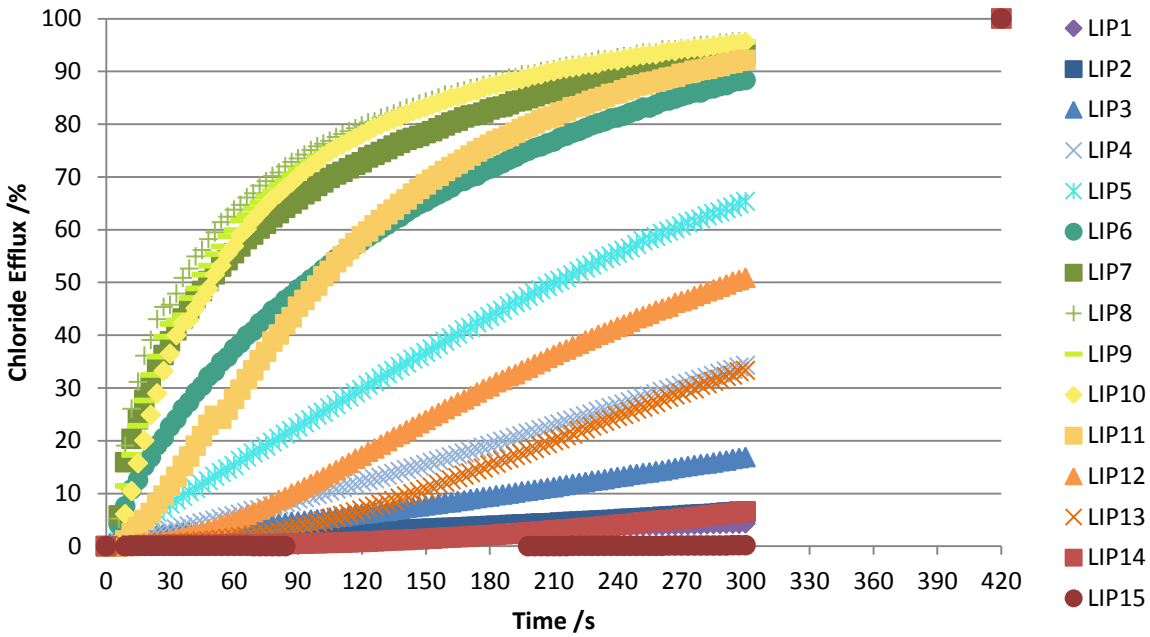


**Figure 39 –** Transport curves for compounds 1-15 in $Cl^-/NO_3^-$ assays in 7:3 POPC:CHOL vesicles. Each curve represents the average of 3 trials.

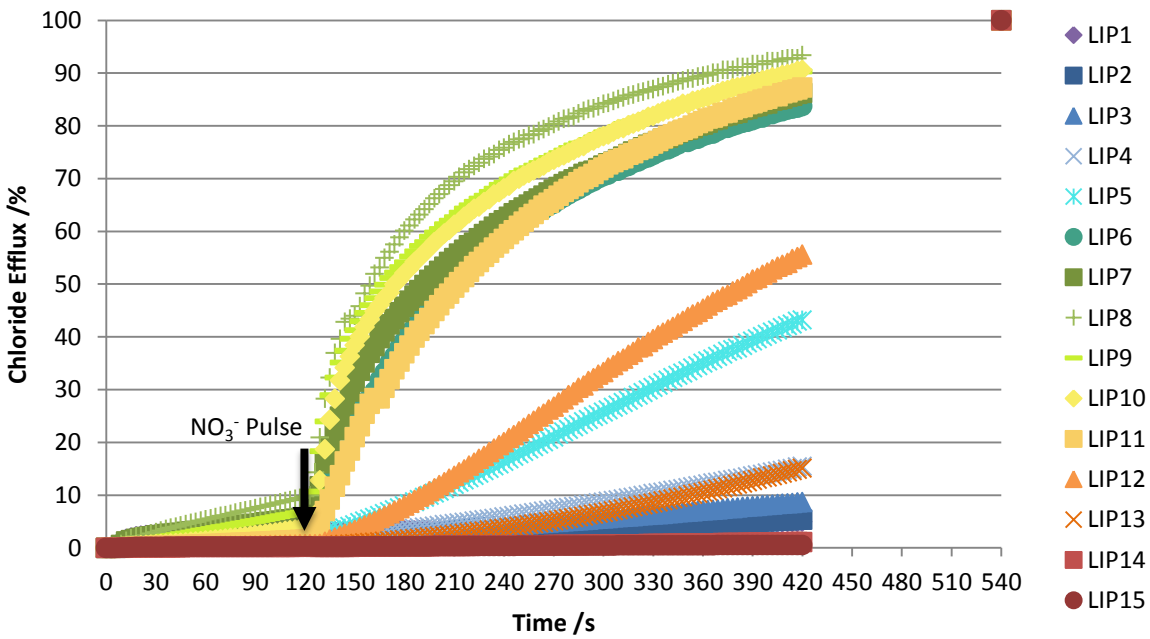


**Figure 40 –** Transport curves for compounds 1-15 in $SO_4^{2-}$ / $NO_3^-$ spike assays in 7:3 POPC:CHOL vesicles. Each curve represents the average of 3 trials.

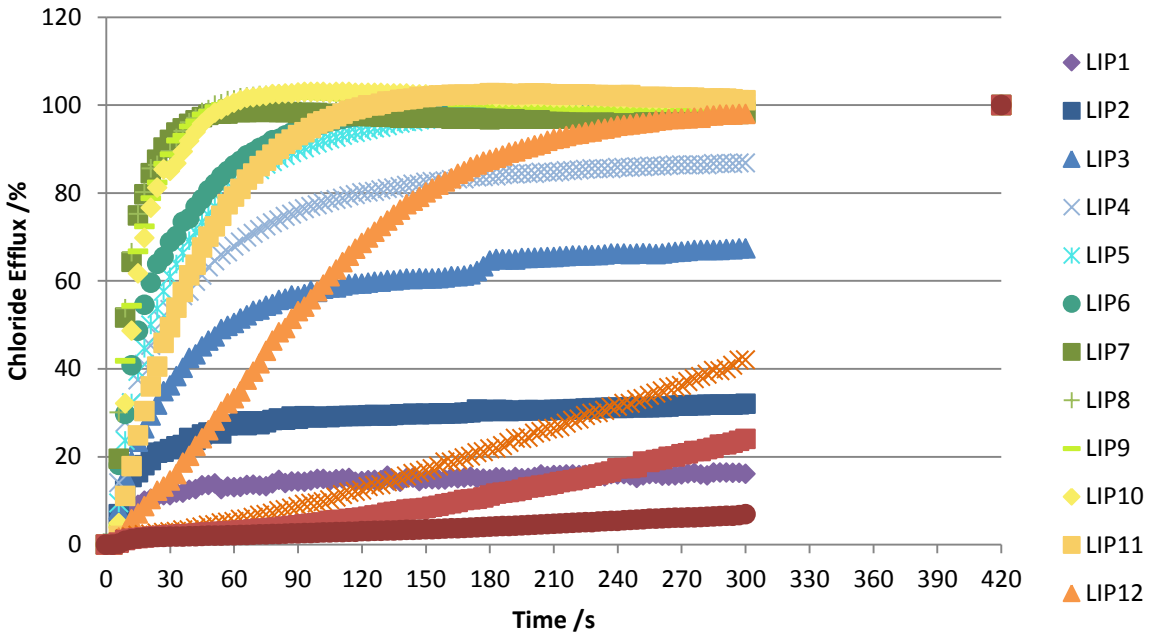


**Figure 41 –** Transport curves for compounds 1-15 in $Cl^-/NO_3^-$ assays in 100% POPC vesicles at 55°C. Each curve represents the average of 3 trials.

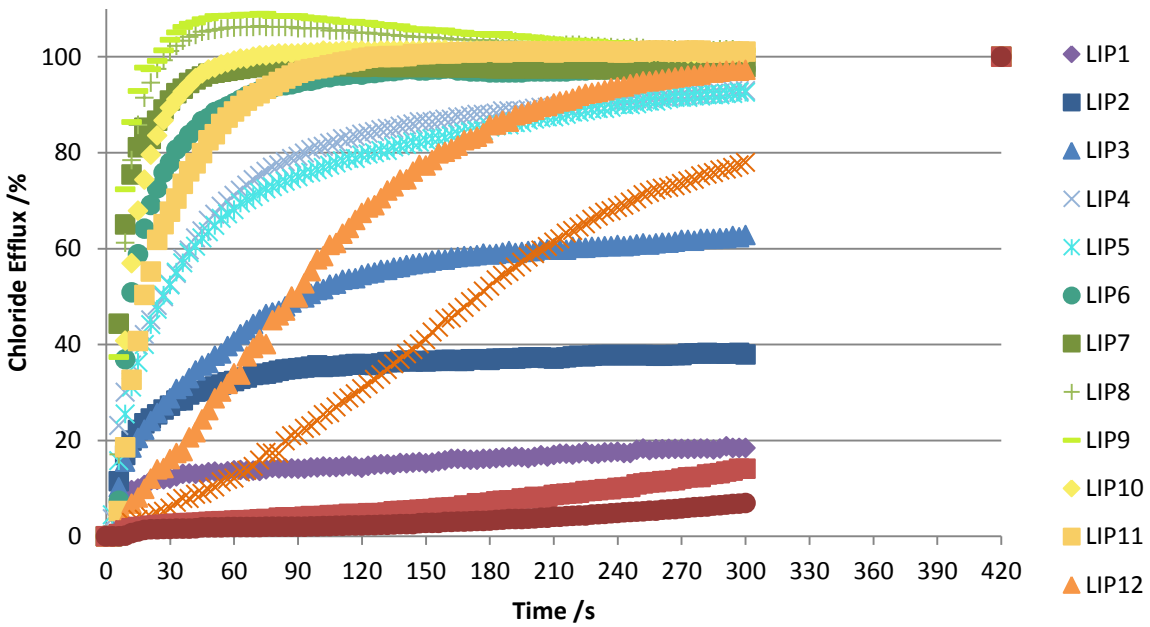


**Figure 42 –** Transport curves for compounds 1-15 in $Cl^-/NO_3^-$ assays in 100% DPPC vesicles at 55°C. Each curve represents the average of 3 trials.

## 5.2 Possible $SO_4^{2-}$ Transport

As much as 30 % chloride efflux was observed for the series before the addition of nitrate in $SO_4^{2-}$/$NO_3^-$ spike assays in the 3:1 POPE:POPC system (Figure 38). Possible explanations of this include general leakage of the vesicles, $SO_4^{2-}$/$Cl^-$ antiport, HCl cotransport or MCl symport.

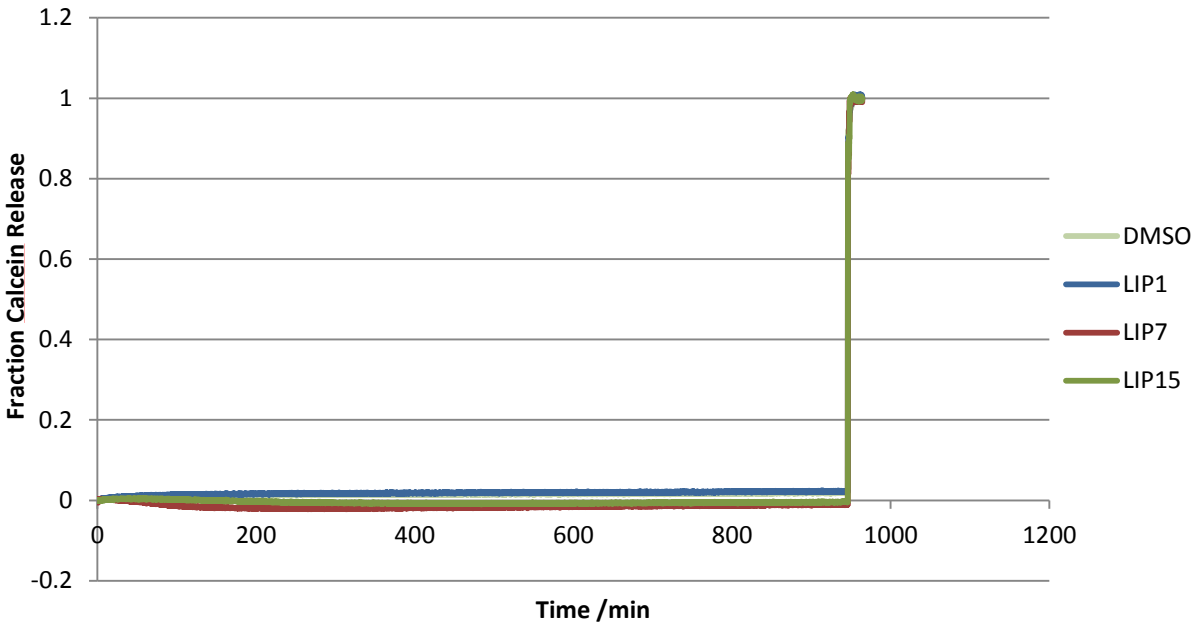


**Figure 43 -** Calcein leakage test for compounds **1**, **7** & **15**

The general leakage of the 3:1 POPE:POPC system was tested by a calcein leakage test. Calcein is a self-quenching fluorophore and an increase in calcein fluorescence is observed with increasing leakage from the vesicles. No significant leakage was observed up to 16 hours after addition of the thioureas.

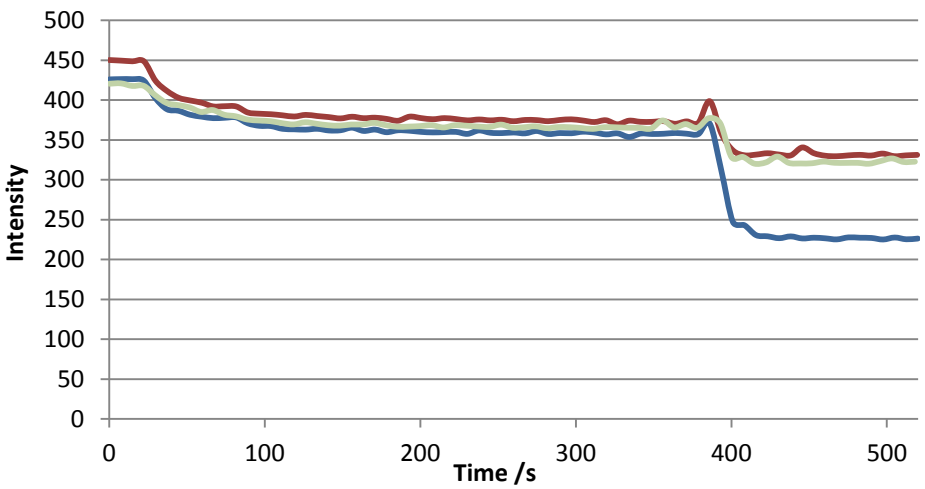


**Figure 44 –** Fluorescence trace (Ex. 372 nm, Em. 503 nm) for lucigenin assay for DMSO. External anion added at 30 s, test compound added at 90 s, vesicles lysed at 390 s. Anion added – Blue: $Cl^-$, Green: $NO_3^-$, Red: $SO_4^{2-}$. Each point represents the average of 3 trials.

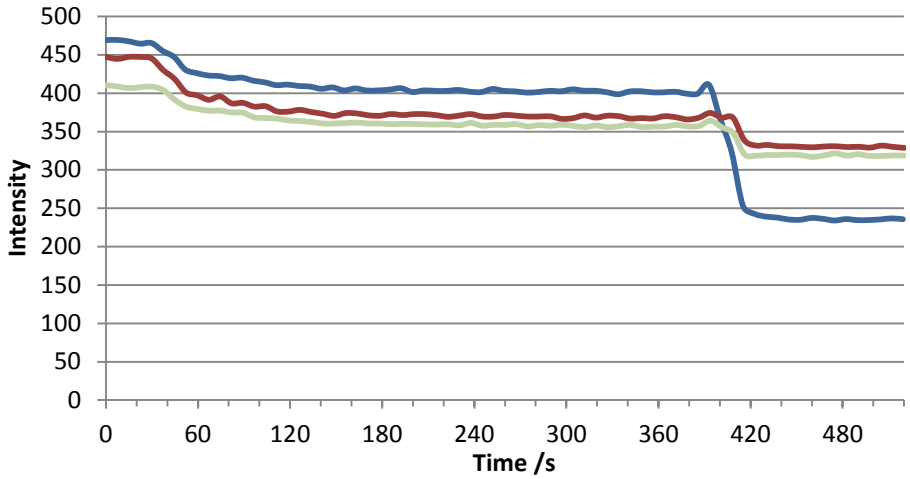


**Figure 45 -** Fluorescence trace (Ex. 372 nm, Em. 503 nm) for lucigenin assay for compound **1**. External anion added at 30 s, test compound added at 90 s, vesicles lysed at 390 s. Anion added – Blue: $Cl^-$, Green: $NO_3^-$, Red: $SO_4^{2-}$. Each point represents the average of 3 trials.

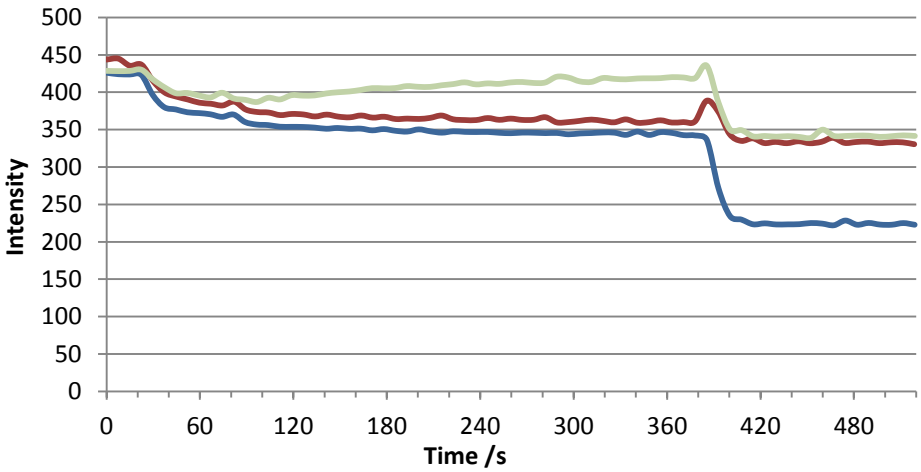


**Figure 46 -** Fluorescence trace (Ex. 372 nm, Em. 503 nm) for lucigenin assay for compound **7**. External anion added at 30 s, test compound added at 90 s, vesicles lysed at 390 s. Anion added – Blue: $Cl^-$, Green: $NO_3^-$, Red: $SO_4^{2-}$. Each point represents the average of 3 trials.

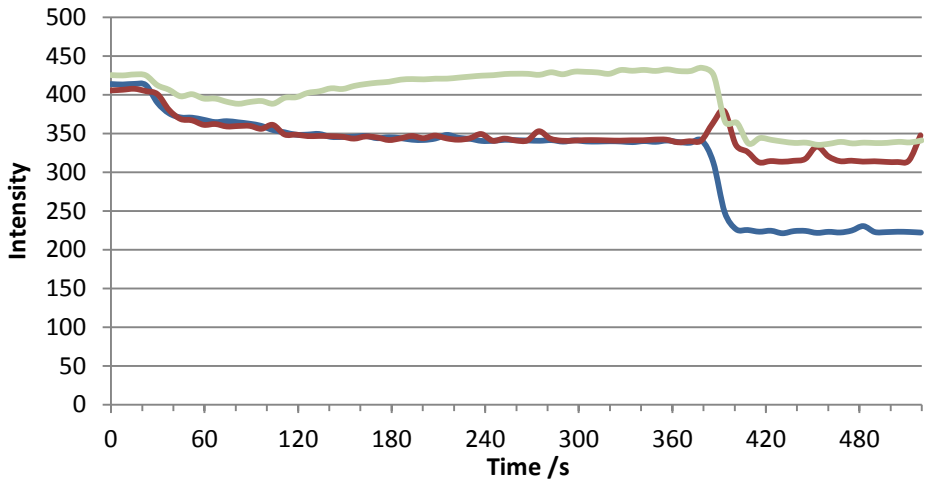


**Figure 47 -** Fluorescence trace (Ex. 372 nm, Em. 503 nm) for lucigenin assay for compound **9**. External anion added at 30 s, test compound added at 90 s, vesicles lysed at 390 s. Anion added – Blue: $Cl^-$, Green: $NO_3^-$, Red: $SO_4^{2-}$. Each point represents the average of 3 trials.

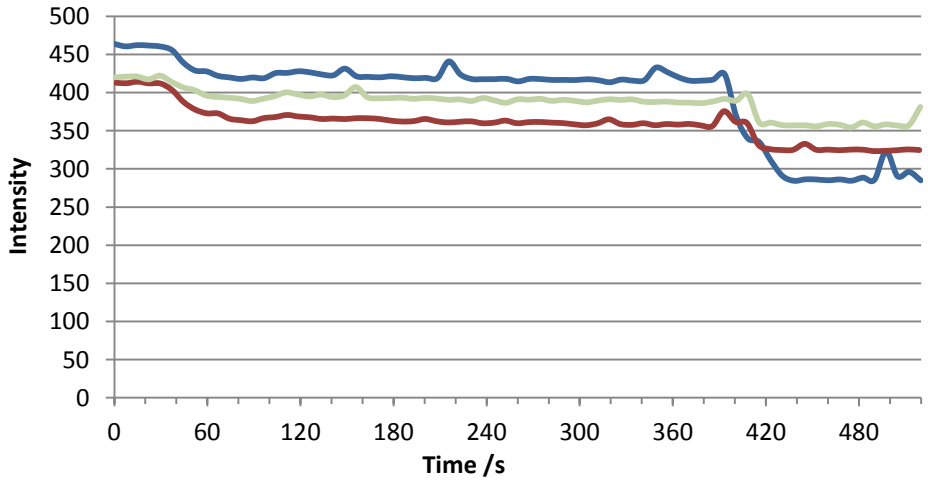


**Figure 48 -** Fluorescence trace (Ex. 372 nm, Em. 503 nm) for lucigenin assay for compound **15**. External anion added at 30 s, test compound added at 90 s, vesicles lysed at 390 s. Anion added – Blue: $Cl^-$, Green: $NO_3^-$, Red: $SO_4^{2-}$. Each trace represents the average of 3 trials.

We attempted to directly observe sulfate transport by a lucigenin assay. Vesicles were prepared containing lucigenin dye and containing $Cl^-$ in both the external and internal medium. During the experiment, a pulse of external anion ($Cl^-$ / $NO_3^-$ / $SO_4^{2-}$) is added, followed 60 s later by the test compound. As lucigenin fluorescence is quenched in the presence of chloride, thus an increase in lucigenin fluorescence after anion addition suggests efflux of chloride from the vesicle, replaced by the added external anion.

In all tests, the change in fluorescence in the presence of external $SO_4^{2-}$ is not significantly different from the $Cl^-$ control. By contrast, the transport of $NO_3^-$ into the vesicle is evident, in line with the relative transport rates observed for each compounds previously. This suggests there is little to no significant sulfate transport in this system.

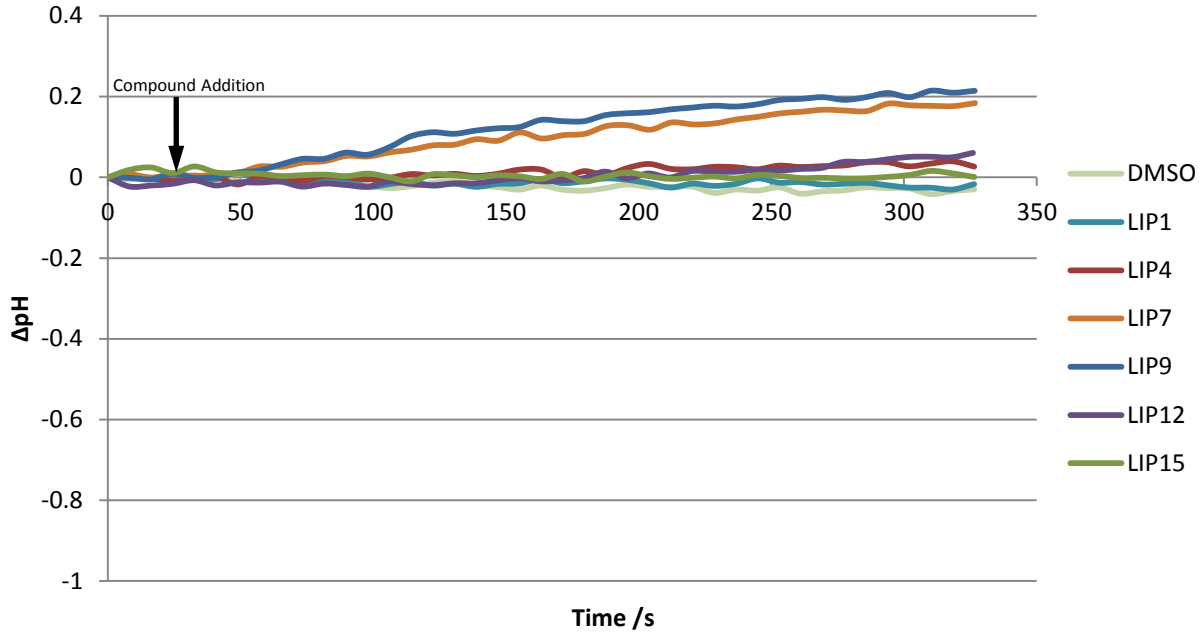


**Figure 49 –** Change in intravesicular pH calculated via HPTS assay. Test compound added at 30 s. Each trace represents the average of 3 trials.

The possibility of HCl cotransport (or $Cl^-$ / $OH^-$ antiport) was tested by monitoring the change in the internal pH of the vesicles. An HPTS assay was used, with the ratio of the fluorescence emissions of the protonated and deprotonated forms converted to a pH value as previously reported[9]. The most active compounds showed a small increase in internal pH over the course of the experiment, indicating that some HCl efflux was possible. However, the magnitude of the pH change is not large enough to fully explain the level of chloride efflux observed in Figure 38 - Transport curves for compounds 1-15 in $SO_4^{2-}$ / $NO_3^-$ spike assays in 3:1 POPE:POPC vesicles. Each curve represents the average of 3 trials. Possible sulfate transport before the addition of nitrate is observed before the addition of nitrate. Mechanisms for this are investigated in section **5.2**.Figure 38.

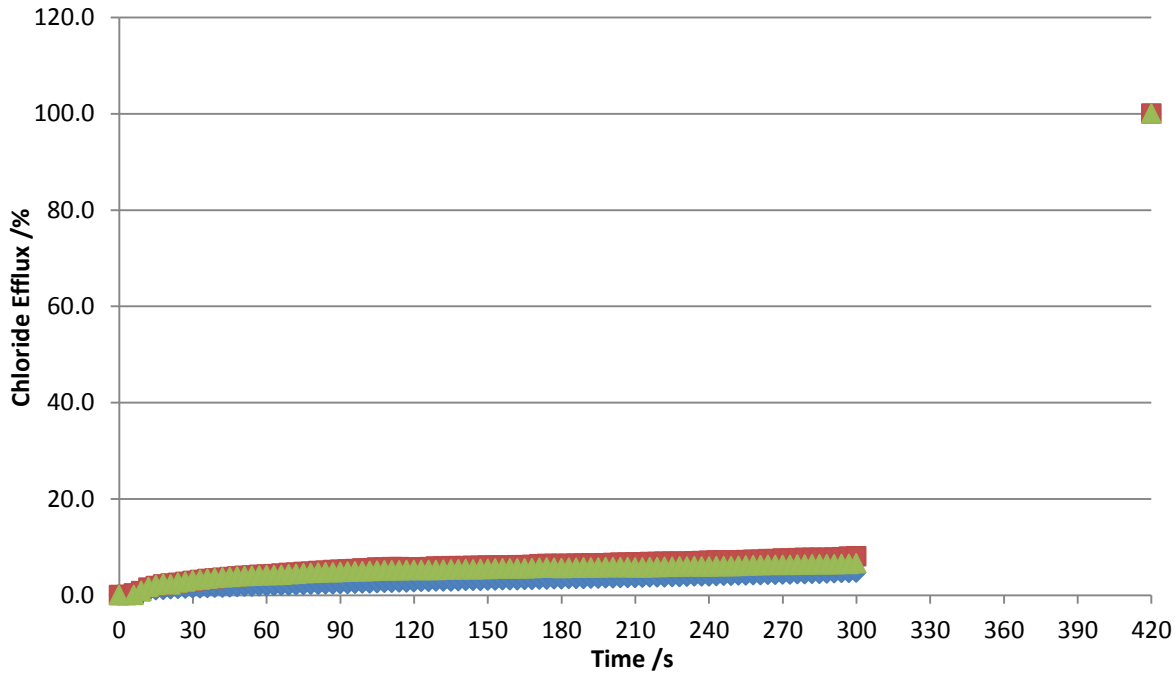


**Figure 50 –** Chloride efflux from 3:1 POPE:POPC vesicles in $Cl^-$ / $NO_3^-$ assays by compound **1** in the presence of varying internal cations. Internal cation - Blue diamonds: $Na^+$, Red squares: $K^+$, Blue Triangles: $Cs^+$. Each point represents the average of 3 trials.

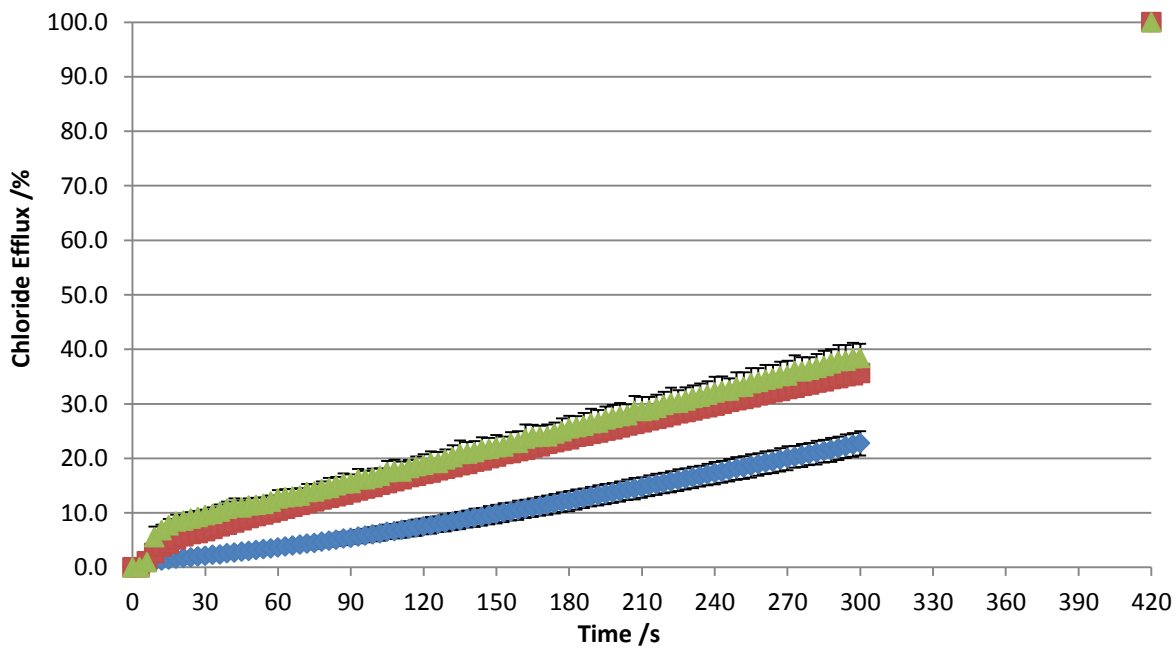


**Figure 51 -** Chloride efflux from 3:1 POPE:POPC vesicles in $Cl^-$ / $NO_3^-$ assays by compound **4** in the presence of varying internal cations. Internal cation - Blue diamonds: $Na^+$, Red squares: $K^+$, Blue Triangles: $Cs^+$. Each point represents the average of 3 trials.

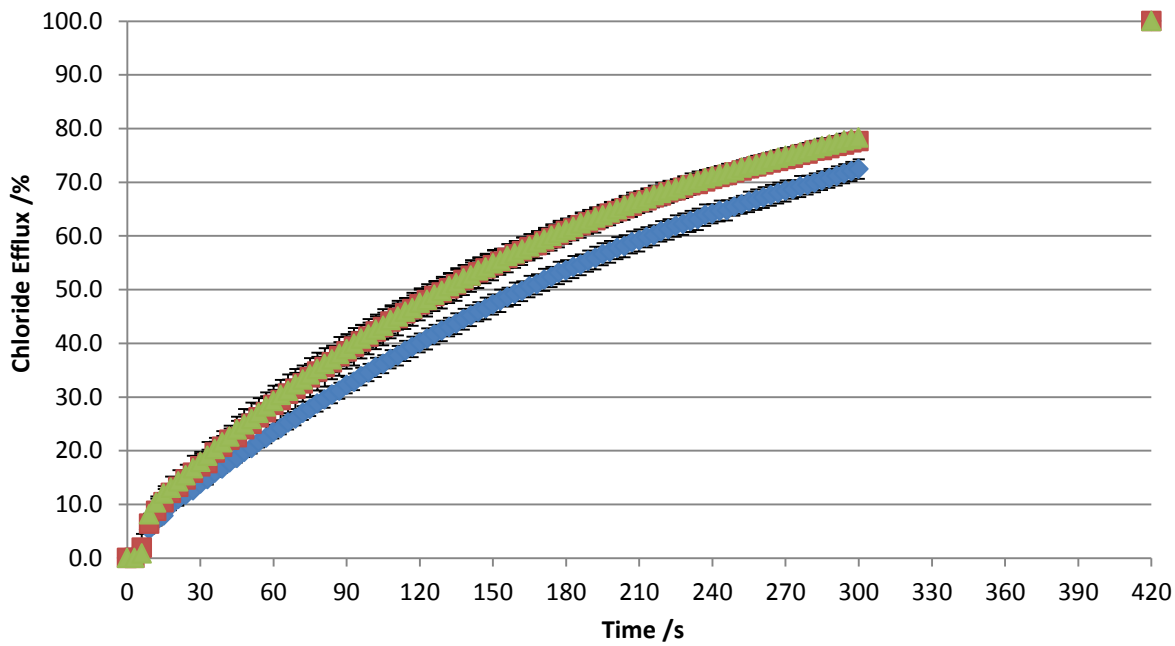


**Figure 52 -** Chloride efflux from 3:1 POPE:POPC vesicles in $Cl^-$ / $NO_3^-$ assays by compound **7** in the presence of varying internal cations. Internal cation - Blue diamonds: $Na^+$, Red squares: $K^+$, Blue Triangles: $Cs^+$. Each point represents the average of 3 trials.

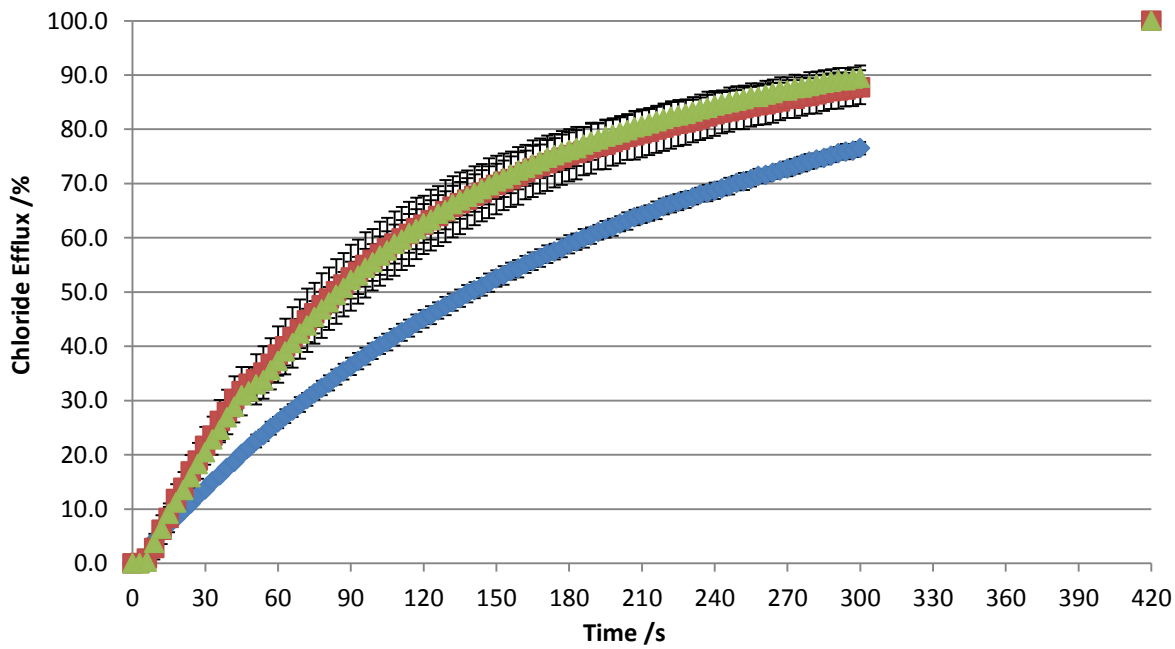


**Figure 53 -** Chloride efflux from 3:1 POPE:POPC vesicles in $Cl^-$ / $NO_3^-$ assays by compound **9** in the presence of varying internal cations. Internal cation - Blue diamonds: $Na^+$, Red squares: $K^+$, Blue Triangles: $Cs^+$. Each point represents the average of 3 trials.

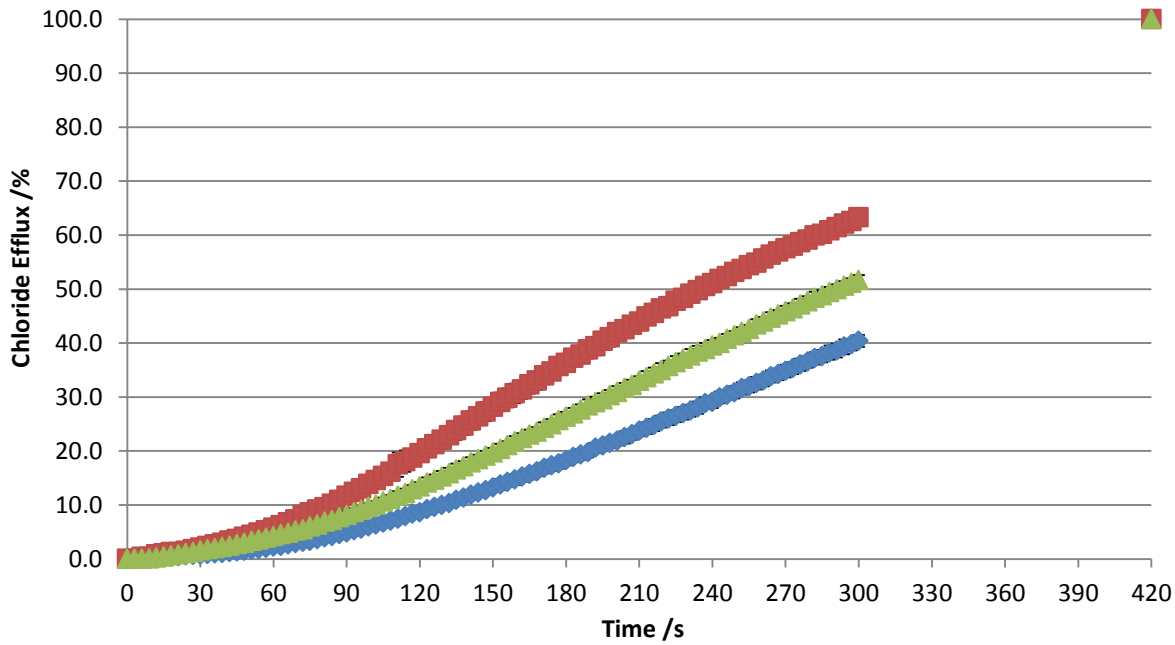


**Figure 54 -** Chloride efflux from 3:1 POPE:POPC vesicles in $Cl^-$ / $NO_3^-$ assays by compound **12** in the presence of varying internal cations. Internal cation - Blue diamonds: $Na^+$, Red squares: $K^+$, Blue Triangles: $Cs^+$. Each point represents the average of 3 trials.

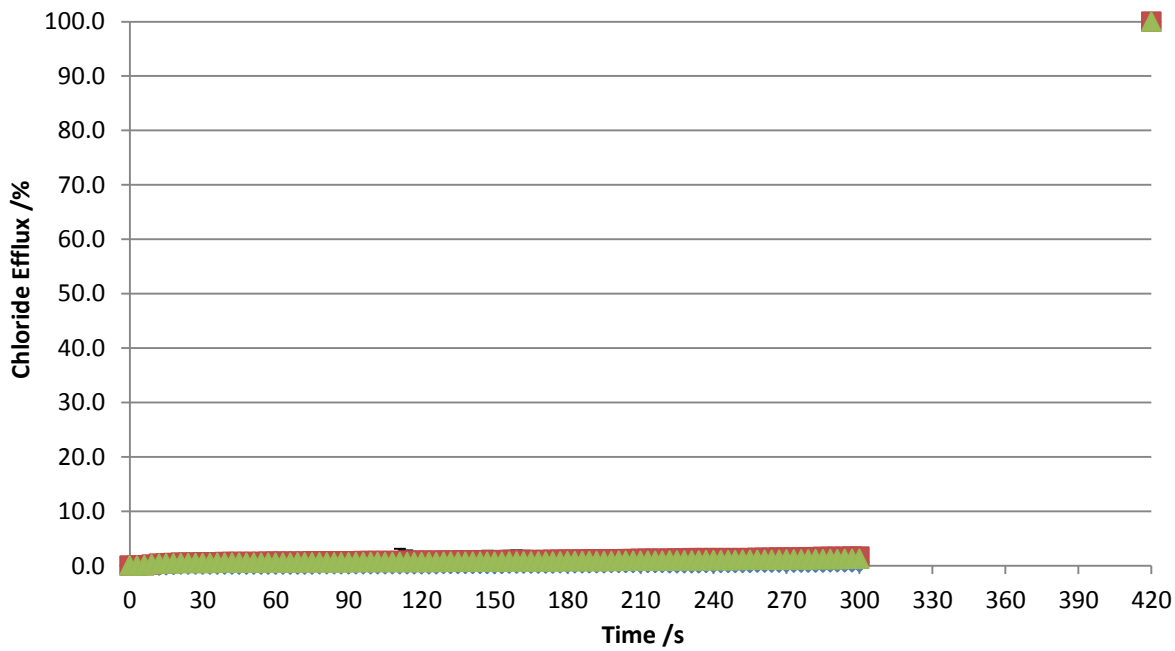


**Figure 55 -** Chloride efflux from 3:1 POPE:POPC vesicles in $Cl^-$ / $NO_3^-$ assays by compound **15** in the presence of varying internal cations. Internal cation - Blue diamonds: $Na^+$, Red squares: $K^+$, Blue Triangles: $Cs^+$. Each point represents the average of 3 trials.

Finally, the dependence on the potential for MCl symport was tested by examining the dependence of transport rate on the internal cation. $Cl^-$ / $NO_3^-$ assays were repeated, replacing the internal salt with KCl and CsCl. It was evident for compounds that were good transporters that the rate of transport was dependent on the cation present. For compounds **7**, **9** & **12**, the larger cations appeared to increase the rate of transport, giving up to 15 % more efflux of chloride after 270 s in the case of compound **9**. This suggests that the compounds are capable of some MCl transport, with the larger cations forming stable ion-pair complexes with the chloride-transporter complex. It is noted that the larger cation appear to decrease the rate for compound **4**, we suggest that they are too large to be shielded from unfavourable interactions with the lipid tail groups by the transporter's shorter alkyl chains.

# 6 NMR Titrations

## 6.1 General Procedure

All salts obtained from Sigma-Aldrich and dried under vacuum overnight prior to use. ~0.01 M solution of the sample receptor produced in 0.5 % $H_2O$/DMSO-$d_6$. 500 µl of initial sample placed in an NMR tube and $^1H$ spectrum recorded using Bruker AVII400 FT-NMR spectrometer at 298 K. Aliquots of an ~0.16 M solution of the TBA (tetrabutyl ammonium) salt of the anionic guest (dissolved in receptor sample solution) were added and $^1H$ NMR spectra obtained for each titre. Approx. 20 spectra obtained spanning 0 to 6 equivalents of anion to receptor. The chemical shift of the alkyl N-H proton over the course of the titration were plotted against the concentration of the anionic guest and the data fitted assuming a 1:1 binding model using WINEQNMR2[10] to obtain the binding constant K. All errors in the calculated values were < 10%, except for when K < 10 (due to a large errors in fitting with small K, these values are reported as K < 10). Although the shift of the aryl N-H proton could also be followed, values are not reported due to peak broadening through the course of the experiment, especially in the presence of TBA $H_2PO_4$.

## 6.2 Fit Plots

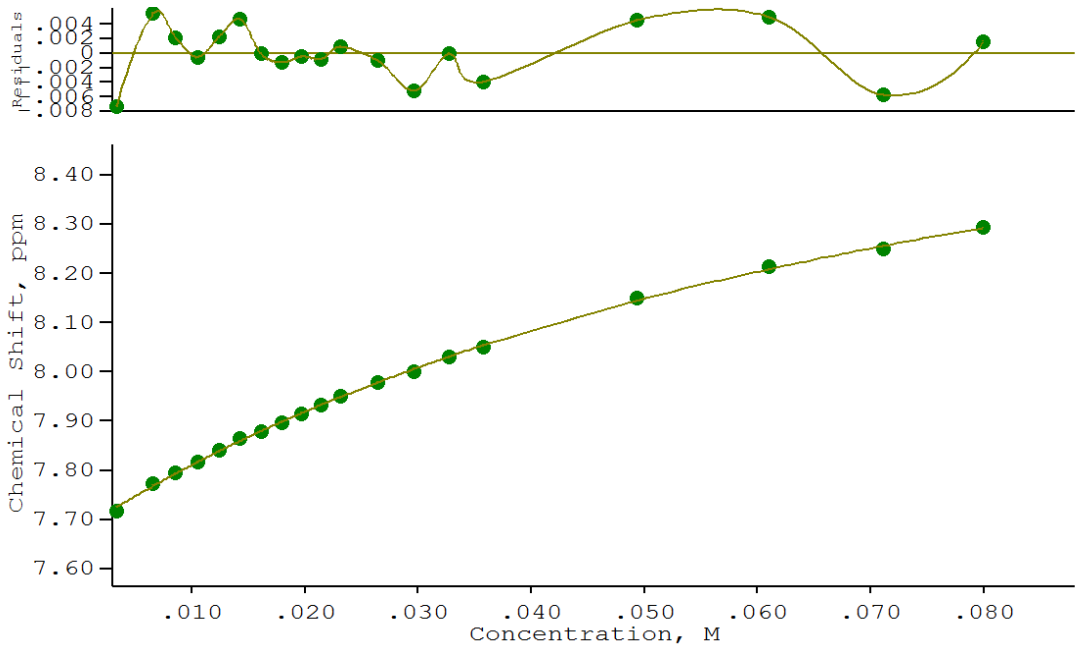


**Figure 56 –** Fit plot for $^1H$ titration of 1-phenyl-3-ethylthiourea with TBA Cl, following the alkyl NH proton (δ = 7.69 ppm). K = 14, error = 4.8 %.

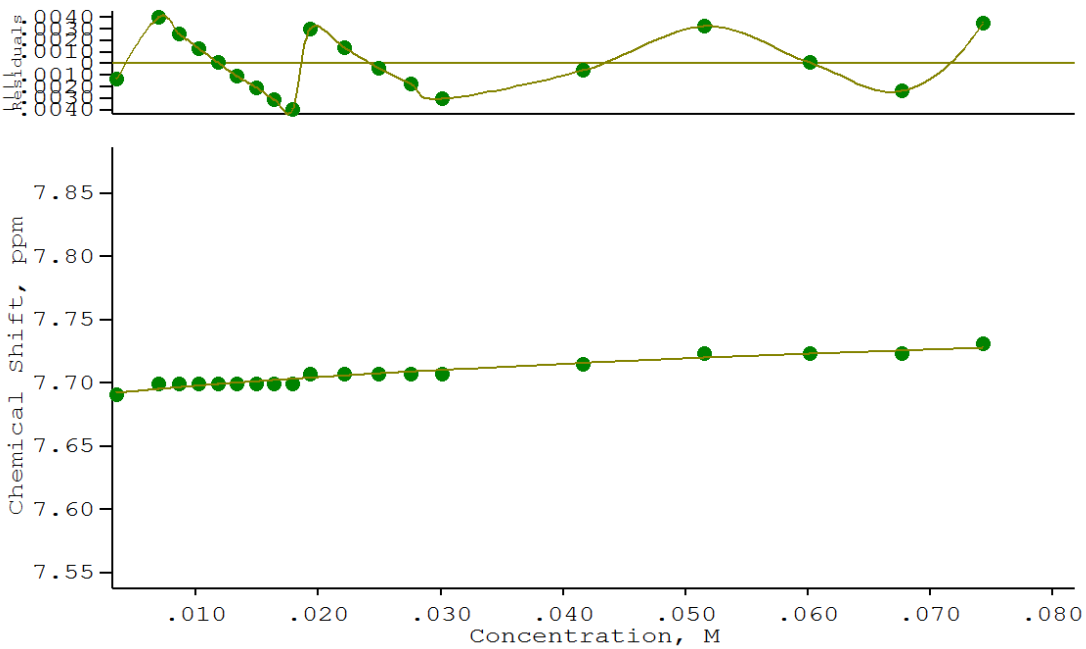


**Figure 57 –** Fit plot for $^{1}$H titration of 1-phenyl-3-ethylthiourea with TBA $NO_3$, following the alkyl NH proton (δ = 7.69 ppm). K < 10.

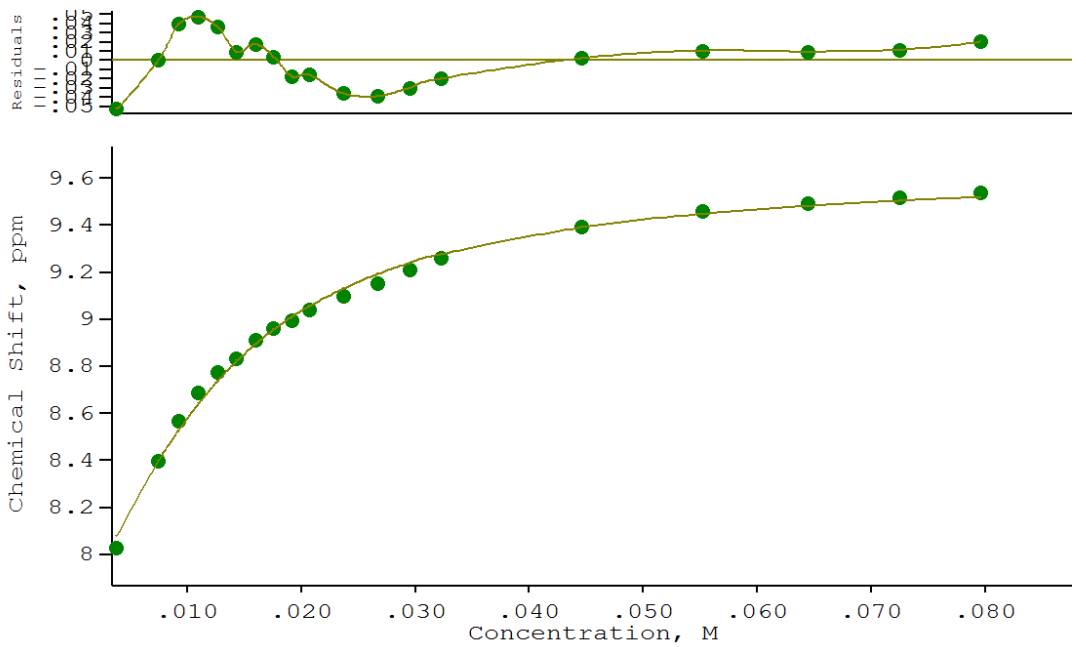


**Figure 58 –** Fit plot for $^{1}$H titration of 1-phenyl-3-ethylthiourea with TBA $H_2PO_4$, following the alkyl NH proton (δ = 7.69 ppm). K = 180, error = 8.5 %.

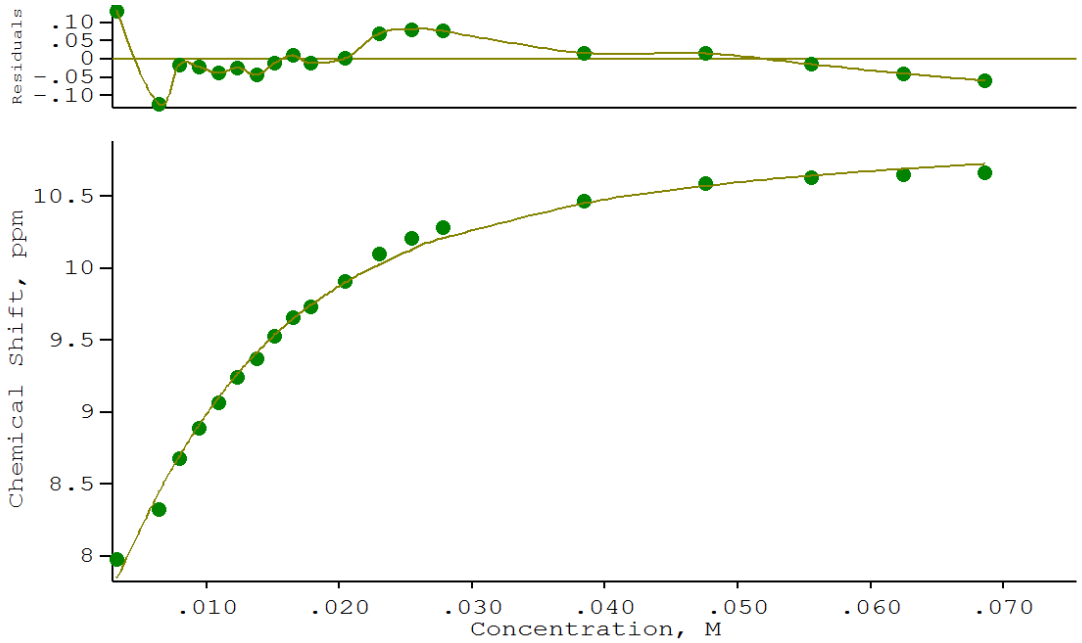


**Figure 59 –** Fit plot for $^{1}H$ titration of 1-phenyl-3-ethylthiourea with $TBA_2\ SO_4$, following the alkyl NH proton (δ = 7.68 ppm). K = 200, error = 9.2 %.

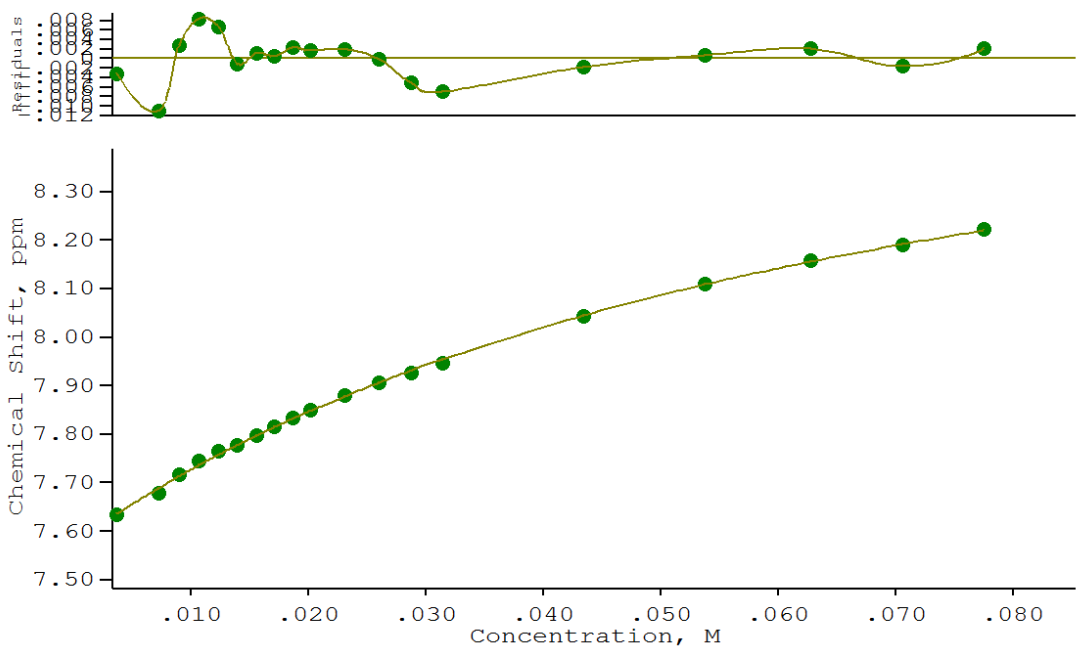


**Figure 60 –** Fit plot for $^{1}H$ titration of 1-(4-butylphenyl)-3-butylthiourea with TBA Cl, following the alkyl NH proton (δ = 7.57 ppm). K = 17, error = 5.6 %.

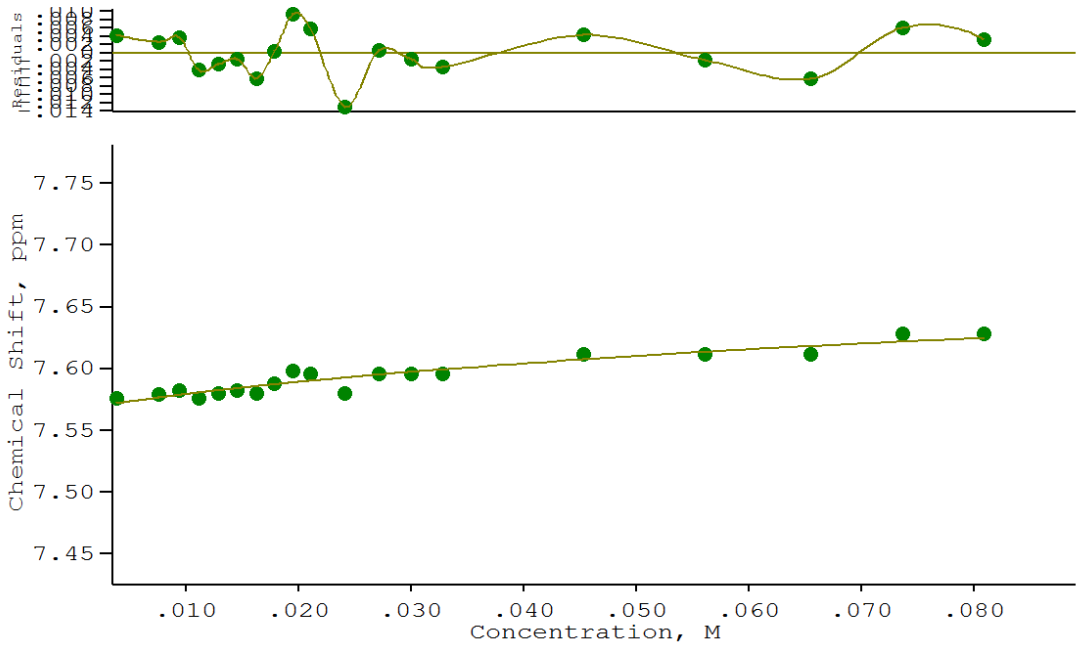


**Figure 61 –** Fit plot for $^{1}$H titration of 1-(4-butylphenyl)-3-butylthiourea with TBA $NO_3$, following the alkyl NH proton (δ = 7.57 ppm). K < 10.

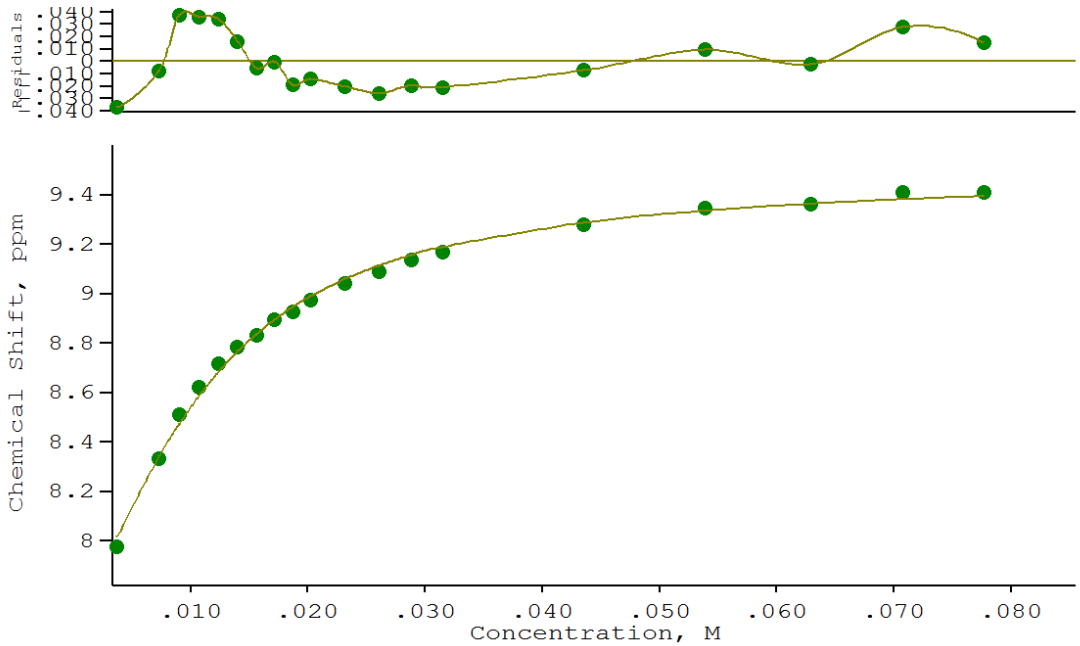


**Figure 62 –** Fit plot for $^{1}$H titration of 1-(4-butylphenyl)-3-butylthiourea with TBA $H_2PO_4$, following the alkyl NH proton (δ = 7.58 ppm). K = 220, error 7.5 %.

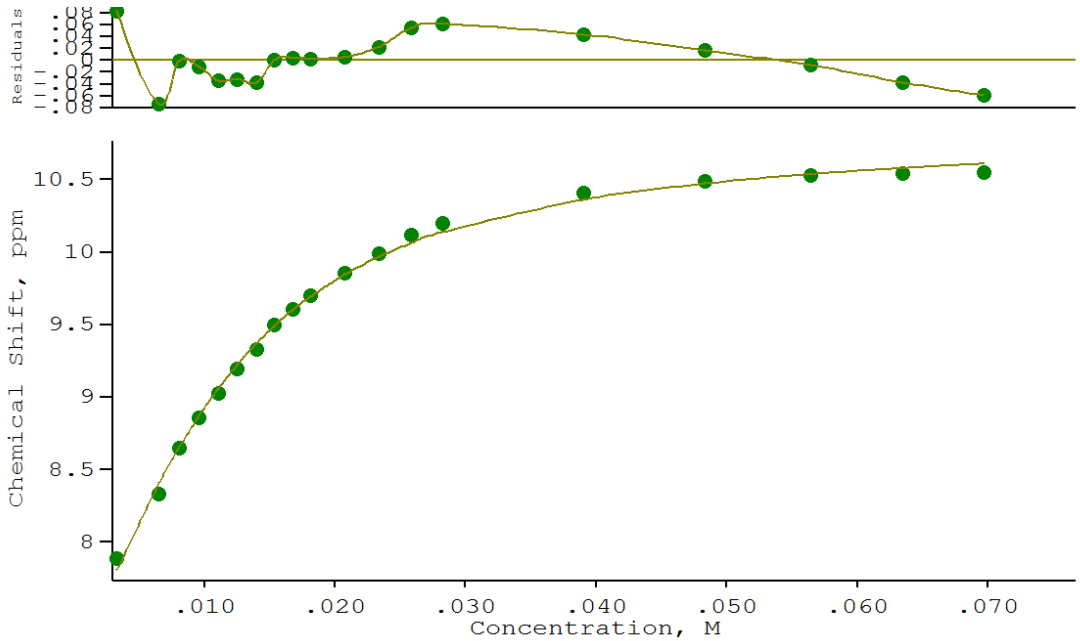


**Figure 63 –** Fit plot for $^{1}$H titration of 1-(4-butylphenyl)-3-butylthiourea with $TBA_2$ $SO_4$, following the alkyl NH proton (δ = 7.57 ppm). K = 220, error = 6.7 %.

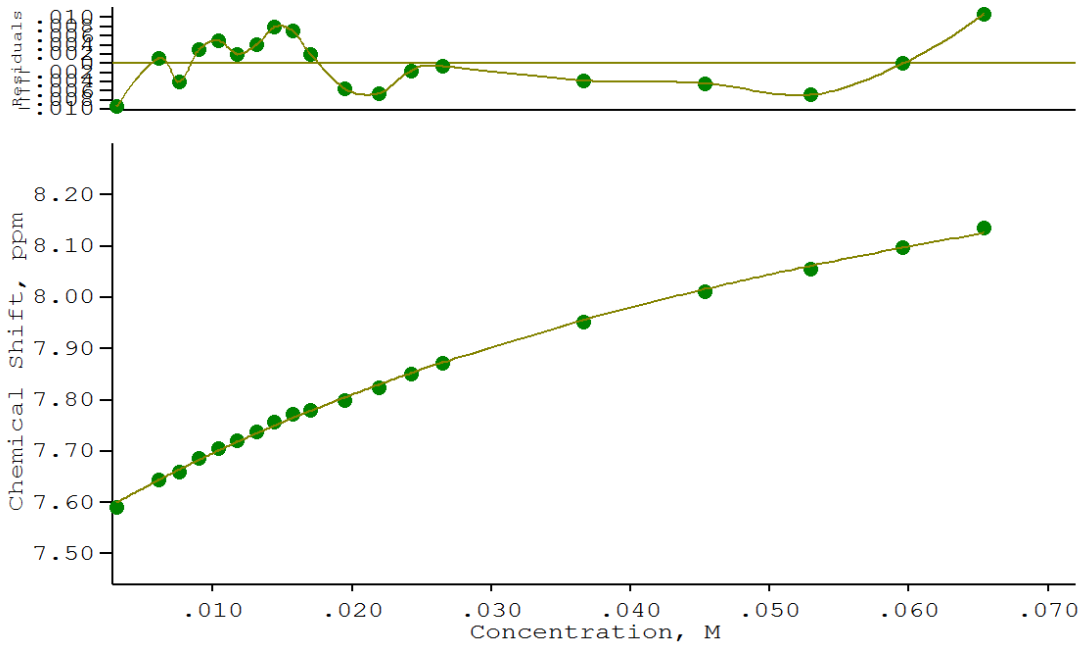


**Figure 64 –** Fit plot for $^{1}$H titration of 1-(4-octylphenyl)-3-octylthiourea with TBA Cl, following the alkyl NH proton (δ = 7.55 ppm). K = 16, error = 8.7 %.

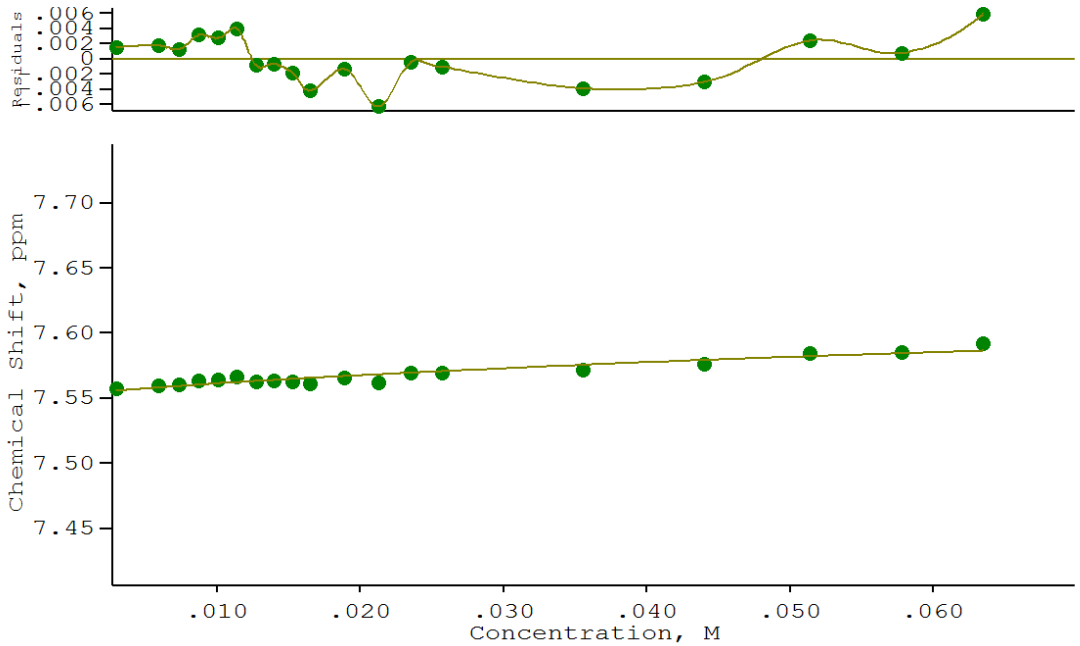


**Figure 65 –** Fit plot for $^{1}$H titration of 1-(4-octylphenyl)-3-octylthiourea with TBA $NO_3$, following the alkyl NH proton (δ = 7.55 ppm). K < 10.

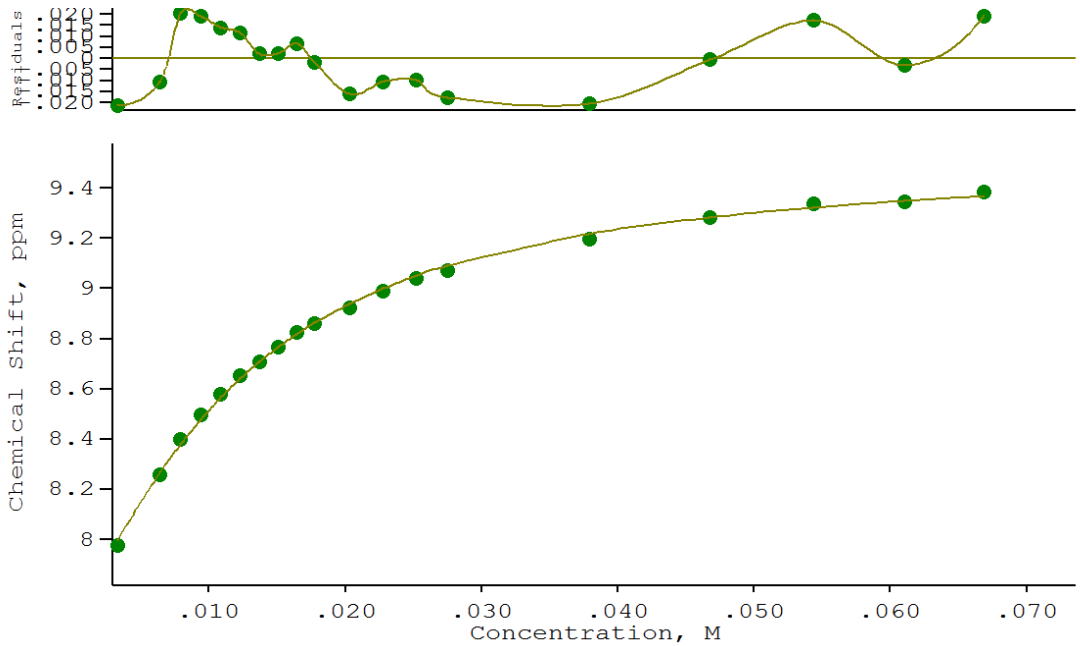


**Figure 66 –** Fit plot for $^{1}$H titration of 1-(4-octylphenyl)-3-octylthiourea with TBA Cl, following the alkyl NH proton (δ = 7.56 ppm). K = 160, error = 4.7 %.

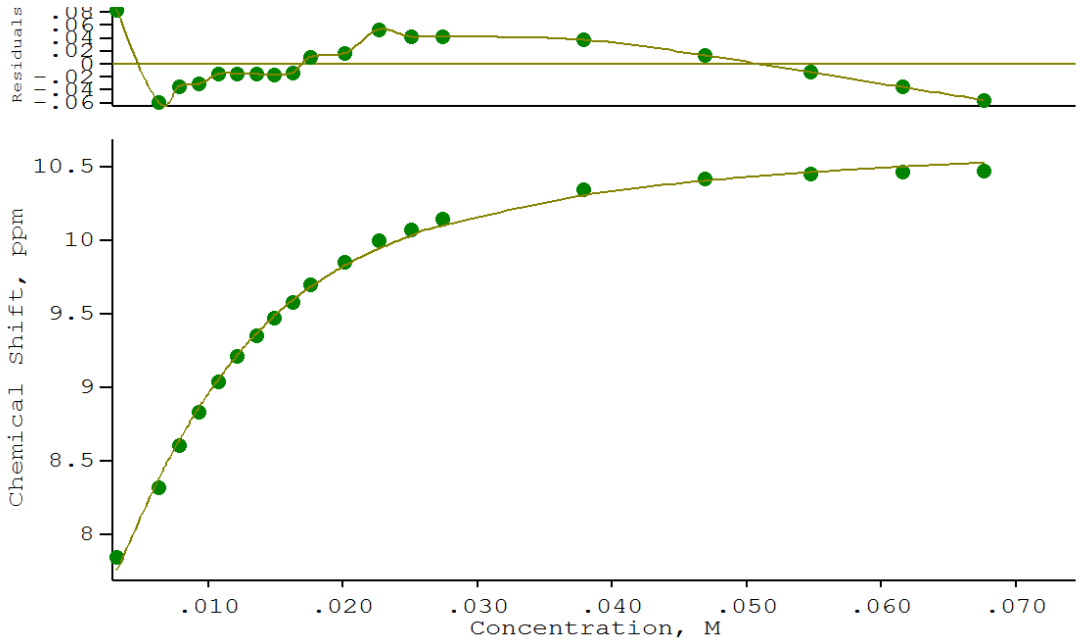


**Figure 67 –** Fit plot for $^{1}$H titration of 1-(4-octylphenyl)-3-octylthiourea with $TBA_2$ $SO_4$, following the alkyl NH proton (δ = 7.56 ppm). K = 250, error = 6.3 %.

# 7 Notes and references


1. W. Weith, *Berichte der deutschen chemischen Gesellschaft*, 1875, **8**, 1523-1530.
2. A. Yahyazadeh and Z. Ghasemi, *Eur. Chem. Bull.*, 2013, **2**, 573-575.
3. N. Busschaert, S. J. Bradberry, M. Wenzel, C. J. E. Haynes, J. R. Hiscock, I. L. Kirby, L. E. Karagiannidis, S. J. Moore, N. J. Wells, J. Herniman, G. J. Langley, P. N. Horton, M. E. Light, I. Marques, P. J. Costa, V. Félix, J. G. Frey and P. A. Gale, *Chem. Sci.*, 2013, **4**, 3036-3045.
4. VCCLAB, Virtual Computational Chemistry Laboratory, http://www.vcclab.org.
5. I. V. Tetko, J. Gasteiger, R. Todeschini, A. Mauri, D. Livingstone, P. Ertl, V. A. Palyulin, E. V. Radchenko, N. S. Zefirov, A. S. Makarenko, V. Y. Tanchuk and V. V. Prokopenko, *J. Comput. Aided Mol. Des.*, 2005, **19**, 453-463.
6. OECD, *OECD Guidelines for the Testing of Chemicals, Section 1*, 2004.
7. A. Berthod and S. Carda-Broch, *J. Chromatogr.*, 2004, **1037**, 3-14.
8. V. Saggiomo, S. Otto, I. Marque, V. Félix, T. Torroba and R. Quesada, *Chem. Commun.*, 2012, **48**, 5274-5276.
9. N. Busschaert, P. A. Gale, C. J. E. Haynes, M. E. Light, S. J. Moore, C. C. Tong, J. T. Davis and J. William A. Harrell, *Chem. Commun.*, 2010, **46**, 6252-6254.
10. M. J. Hynes, *J. Chem. Soc., Dalton Trans.*, 1993, 311-312.